

ISTANBUL TECHNICAL UNIVERSITY ★ GRADUATE SCHOOL OF SCIENCE
ENGINEERING AND TECHNOLOGY

**EFFECT OF INTERMEDIATE DEFORMATION ON FORMABILITY
PARAMETERS OF RETROGRESSION AND REAGED (RRA) 7075 ALLOY**

M.Sc. THESIS

Armin RASHIDI

Department of Metallurgy and Material Engineering

Materials Programme

MAY 2015

ISTANBUL TECHNICAL UNIVERSITY ★ GRADUATE SCHOOL OF SCIENCE
ENGINEERING AND TECHNOLOGY

**EFFECT OF INTERMEDIATE DEFORMATION ON FORMABILITY
PARAMETERS OF RETROGRESSION AND REAGED (RRA) 7075 ALLOY**

M.Sc. THESIS

**Armin RASHIDI
(506101433)**

Department of Metallurgy and Material Engineering

Materials Programme

Thesis Advisor: Assoc. Prof. Dr. Murat BAYDOĞAN

MAY 2015

İSTANBUL TEKNİK ÜNİVERSİTESİ ★ FEN BİLİMLERİ ENSTİTÜSÜ

**RETROGRESYON VE YENİDEN YAŞLANDIRMA (RRA) UYGULANMIŞ 7075
ALAŞIMININ ŞEKİLLENDİRİLEBİLİRLİK PARAMETRELERİNE ARA
DEFORMASYON İŞLEMİNİN ETKİSİ**

YÜKSEK LİSANS TEZİ

**Armin RASHIDI
(506101433)**

Metalurji ve Malzeme Mühendisliği Anabilim Dalı

Malzeme Mühendisliği Programı

Tez Danışmanı: Doç. Dr. Murat BAYDOĞAN

MAYIS 2015

Armin-RASHIDI, a M.Sc. student of ITU **Institute of GRADUATE SCHOOL OF SCIENCE ENGINEERING AND TECHNOLOGY** student ID **506101433**, successfully defended the **thesis** entitled “**EFFECT OF INTERMEDIATE DEFORMATION ON FORMABILITY PARAMETERS OF RETROGRESSION AND REAGE (RRA) 7075 ALLOY**”, which he prepared after fulfilling the requirements specified in the associated legislations, before the jury whose signatures are below.

Thesis Advisor : **Assoc. Prof. Dr. Murat BAYDOĞAN**
Istanbul Technical University

Jury Members : **Prof. Dr. Hüseyin ÇİMENÖĞLU**
Istanbul Technical University

Assoc. Prof.Dr. Erdem ATAR
Gebze Technical University

Date of Submission : 4 May 2015
Date of Defense : 28 May 2015

To my family,

FOREWORD

I would like to thank my supervisor Assoc.Prof.Dr. Murat BAYDOĞAN for his valuable times, comments and guidance throughout my thesis.

I wish to express my deepest gratitude to my father and my mother, Manouchehr RASHIDI and Robabe SAEIDI, for their sacrifices throughout my life and for their endless love, support, encouragement, and inspiration. Lots of gratitude also goes to my dear wife Nazila MOLAVIZADEH, who backs up for me anytime and anywhere and I want to express my deepest gratitude for his support and endless love. To my brothers Arash, Farid and Aidin for their love and support.

Also, I would like to thank research assistant Yakup YÜREKTÜRK. This thesis would not have been possible without all their help and support.

May 2015

Armin RASHIDI
(Civil Engineer)

TABLE OF CONTENTS

	<u>Page</u>
FOREWORD	ix
TABLE OF CONTENTS	xi
ABBREVIATIONS	xiii
LIST OF TABLES	xv
LIST OF FIGURES	xvii
SUMMARY	xix
ÖZET	xxiii
1. INTRODUCTION	1
2. ALUMINUM AND ALUMINUM ALLOYS	3
2.1 History of Aluminum	3
2.2 Physical Properties of Aluminum	3
2.2.1 Atomic structure of aluminum	3
2.2.2 Crystal structure	4
2.3 Classification of Aluminum Alloys	5
2.3.1 Temper designations of non heat-treatable aluminum alloys	7
2.3.2 Temper designations of heat-treatable aluminum alloys	9
2.4 Physical, Mechanical and Corrosion Properties of Aluminum Alloys	11
2.4.1 Work hardening	11
2.4.2 Dispersion hardening	12
2.4.3 Solid solution hardening	12
2.4.4 Precipitation hardening	13
2.4.5 Electrical conductivity and resistivity of aluminum	14
2.4.6 Tensile strength	14
2.4.7 Proof stress	15
2.4.8 Elastic properties	16
2.4.9 Hardness	16
2.4.10 Corrosion resistance	17
2.5 Comparison of Aluminum Alloys	17
2.6 7075 Aluminum Alloy	19
2.6.1 Effect of age hardening on microstructure and mechanical properties of 7075-T6 Aluminum alloys	22
3. RETROGRESSION AND REAGING (RRA) HEAT TREATMENT	25
3.1 Introduction	25
3.2 Process	25
3.3 Effect of RRA on Microstructure	26
3.3.1 Effect of RRA on fractograph	30
3.3.2 Effect of retrogression time on microstructure	31
4. EXPERIMENTAL PROCEDURE	33
4.1 Material	33
4.2 Retrogression and Reaging Heat Treatment	33

4.3 Intermediate Deformations and Tensile Test.....	34
4.4 Hardness Tests.....	36
4.5 Electrical Conductivity Measurements.....	36
5. EXPERIMENTAL RESULTS AND DISCUSSION	37
5.1 Tensile Tests	37
5.1.1 Result of ultimate tensile strength, yield strength and elongation	37
5.1.2 Result of strain hardening exponent (n).....	41
5.1.2.1 Effect of intermediate deformation	41
5.1.2.2 Effect of rolling orientation	42
5.1.2.3 Effect of temperature.....	45
5.1.3 Result of anisotropy coefficient (R).....	47
5.2 Hardness tests	48
5.3 Electrical Conductivity Measurements.....	49
5.4 Comparison of Experimental Results of 7075-T6 and 7075-RRA Alloys.....	49
6. CONCLUSION.....	51
REFERENCES	53
CURRICULUM VITAE	57

ABBREVIATIONS

RRA	: Retrogression and Reaging
ASTM	: American Society for Testing and Materials
ASM	: American Society for Metals
TEM	: Transmission Electron Microscopy
SEM	: Scanning Electron Microscopy
SCC	: Stress Corrosion Cracking
UTS	: Ultimate Tensile Strength
GISS	: Gas Induced Semi-Solid
N	: Tensile Strain Hardening Exponent
R	: Anisotropy Coefficient

LIST OF TABLES

	<u>Page</u>
Table 2.1 : The main tempers in use for structural application of precipitation hardened semi products.....	11
Table 2.2 : Comparison of mechanical properties for T0 and T6 tempers	20
Table 4.1 : Chemical composition of the studied 7075-T6 alloy	33
Table 4.2 : Experimental layout for intermediate deformation	34
Table 5.1 : Comparison of mechanical test results	50

LIST OF FIGURES

	<u>Page</u>
Figure 2.1 : Aluminum crystal structure	4
Figure 2.2 : Atomic structure of aluminum.....	4
Figure 2.3 : Classification of aluminum alloys	5
Figure 2.4 : Aluminum alloy designatio system	7
Figure 2.5 : A selection of common temper designations for aluminum alloys	9
Figure 2.6 : Work hardening of aluminum.	12
Figure 2.7 : Metallurgy of precipitation hardening (e.g Al -Cu System).....	13
Figure 2.8 : Stress-strain curves of aluminum in comparison with various metals and alloys.....	15
Figure 2.9 : Plastic yield behavior of aluminum and mild steel	15
Figure 2.10 : Pitting corrosion behavior of 3103 mill finis aluminum sheet	17
Figure 2.11 : The Effect of Alloying Elements on Tensile Strength, Hardness, impact sensitivity and ductility.....	18
Figure 2.12 : The effect of alloying elements on weldability and anodising.....	18
Figure 2.13 : The effects of alloying elements on corrosion resistance and fatigue strength	18
Figure 2.14 : The effect of alloying elements on density and young's modulus	19
Figure 2.15 : SEM micrograph of AA7075-T6 alloy.....	20
Figure 2.16 : Hardness vs. time for various aging temperatures.....	22
Figure 2.17 : Tensile strength and % elongation of GISS-processed rheocasting 7075 Al alloy after T6 aging process at various temperatures and time durations....	23
Figure 2.18 : TEM bright field imaging in [0 1 1] zone axis of specimen aged at (a) 120 ⁰ C for 24 h; and in [1 1 4] zone axis of specimens aged at (b) 120 ⁰ C for 72 h (c) 145 ⁰ C for 6 h (d) 165 ⁰ C for 3 h (e) 185 ⁰ C for 1 h and (f) 185 ⁰ C for 12h..	23
Figure 3.1 : Thermal cycle diagram of the two-step retrogression and reaging treatment after T6 temper..	26
Figure 3.2 : TEM bright field micrographs within grain for (a) 7075-T6 alloy and (b) 7075-RRA alloy	29
Figure 3.3 : TEM microstructure of the T6 temper.....	29
Figure 3.4 : TEM microstructure after retrogression at 200 ⁰ C.....	30
Figure 3.5 : TEM microstructure after RRA (retrogression at 180 ⁰ C).	30
Figure 3.6 : SEM fractographs of alloy after (a) T6 and (b) RRA treatments.	31
Figure 3.7 : Microstructural evaluation of the alloys after retrogression and RRA	32
Figure 5.1 : Variation of strength and elongation at fracture of the samples retrogressed at 220 ⁰ C and then reaged as a function of intermediate deformation for different orientations.	37

Figure 5.2	: Variation of strength and elongation at fracture of the samples retrogressed at 250°C and then reaged as a function of intermediate deformation for different orientations.	38
Figure 5.3	: Variation of strength and elongation at fracture of the samples retrogressed at 280°C and then reaged as a function of intermediate deformation for different orientations.	38
Figure 5.4	: Variation of yield strength as a function of retrogression temperature for different intermediate deformations and orientations.	39
Figure 5.5	: Variation of ultimate tensile strength as a function of retrogression temperature for different intermediate deformations and orientations.....	40
Figure 5.6	: Variation of elongation at fracture as a function of retrogression temperature for different intermediate deformations and orientations	40
Figure 5.7	: Variation of strain hardening exponent as a function of intermediate deformations at different retrogression temperatures for the sample orientations of (a) 0°, (b) 45° and (c) 90°.....	41
Figure 5.8	: Variation of strain hardening exponent as a function of intermediate deformations for different sample orientations for the samples retrogressed at (a) 220°C, (b) 250°C and (c) 280°C.....	42
Figure 5.9	: Variation of strain hardening exponent with respect to sample orientation for different intermediate deformations for the samples retrogressed at (a) 220°C, (b) 250°C and (c) 280°C.....	43
Figure 5.10	: Variation of strain hardening exponent with respect to sample orientation for different retrogression temperatures for the intermediate deformations of (a) 0% (undeformed), (b) 2%, (c) 4%, (d) 6% (e) RRA2%.	44
Figure 5.11	: Variation of strain hardening exponent with respect to retrogression temperature for different intermediate deformations for the sample orientations of (a) 0°, (b) 45° and (c) 90°	45
Figure 5.12	: Variation of strain hardening exponent with respect to retrogression temperature for different sample orientations for the intermediate deformations of (a) 0% (undeformed), (b) 2%, (c) 4%, (d) 6% (e) RRA2%.....	46
Figure 5.13	: Variation of anisotropy coefficient with respect to sample orientation for different retrogression temperatures for the intermediate deformations of (a) 0% (undeformed), (b) 2%, (c) 4%, (d) 6% (e) RRA2%.....	47
Figure 5.14	: Variation of anisotropy coefficient as a function of intermediate deformation for different retrogression temperatures for the sample orientations of (a) 0°, (b) 45° and (c) 90°.....	48
Figure 5.15	: Variation of hardness with respect to intermediate deformation for different retrogression temperatures.	48
Figure 5.16	: Variation of electrical conductivity with respect to intermediate deformation for different retrogression temperatures.....	49

EFFECT OF INTERMEDIATE DEFORMATION ON FORMABILITY PARAMETERS OF RETROGRESSION AND REAGED (RRA) 7075 ALLOY

SUMMARY

High-strength age-hardened 7xxx series Al–Zn–Mg–Cu alloys are widely used for aircraft structures, where they are subjected to demanding operating conditions. Important properties that must be considered for these applications are strength, ductility, corrosion resistance and damage tolerance (e.g. fracture toughness and fatigue resistance). Even though 7075 aluminum alloy was developed over 70 years ago, many researches still have been performed on it in the past decade. 7xxx series alloys have zinc as their main alloying element, often with significant amounts of copper and magnesium. They can be strengthened through precipitation hardening treatment which is designated by T6 temper.

T6 heat treatment is a major heat treatment to enhance mechanical properties of the alloy which can be achieved through an optimization of both solution heat treatment and artificial aging parameters. Wrought 7075-T6 Al alloy is a precipitation-hardened alloy that possesses excellent mechanical properties at temperatures between 25 and 100°C. Its tensile strength sharply decreases with increasing temperature at temperatures above 100°C.

RRA (retrogression and reaging) heat treatment is capable of producing a material with mechanical strength and stress corrosion resistance higher than those presented by the T6 temper. This is true even for a lower range of retrogression temperatures (from 160° to 220°C) than that recommended in the literature (220°-280°C). RRA consists of applying to the alloy in the T6 temper a double stage thermal cycle: The first stage (retrogression stage) runs at higher temperature and is followed by a stage similar to that used to obtain the T6 temper (re-aging stage).

The heat treatment process of RRA for 7075 alloy involves a material being heated to a high temperature just below the solvus line for a short period of time in a salt bath and after that, sample is quenched in cold water. This step of the process is

called retrogression. The material is then reaged for 24 hours at 120°C to give it its peak strength.

Even though retrogression should be carried out at a temperature below the solvus line of the alloy, but it should be high enough to allow for the partial or complete dissolution of GP zones and fine η' (MgZn_2) precipitates.

The microstructure resulting from the RRA is fine η' precipitates within the grains similar to the T6 condition and η precipitates distribution at the grain boundaries similar to the T7 temper. This combination of the microstructure can improve corrosion resistance without strength loss. The high density of fine precipitates is responsible for the high strength, η precipitates at the grain boundaries are responsible for high corrosion resistance.

For Al–Zn–Mg–Cu (7xxx) alloys, retrogression is responsible for the dissolution of the less stable constituents microstructural (GP zones and the finer particles of η') inside the grains, and re-aging promotes the re-precipitation of η' whilst its pre-existent particles grow and transform to η . Hence a retrogression and reaging process can increase the difference of size, spacing and distribution between grain and grain boundary precipitates.

The material used in this study is a commercial 7075-T6 aluminum alloy (Al–Zn–Mg–Cu alloy). It was received in the form of sheet with the dimensions of 2000 mm x 1000 mm x 2 mm (l x w x t). The alloy has been given T6 temper. Commercial heat treatment procedure for T6 temper is solution treatment at 475°C for 30 min., quenched in water, and then artificially aged at 120°C for 24 h. Tensile test samples were cut from the plate in different orientations such as 0°, 45° and 90° to the rolling direction.

In order to investigate effect of intermediate deformation on strength and formability parameters of RRA treated alloy, tensile tests were applied to determine yield strength, ultimate tensile strength, tensile strain hardening exponents (n -values) and anisotropy coefficient (R values).

Results show that for all rolling orientations, yield and tensile strength of RRA samples decrease with respect to those of T6 tempered sample. On the other hand, the sample retrogressed at 250°C has the highest UTS and yield strength, while

220°C and 280°C have nearly similar UTS and yield strength. In the view point of high strength, it is determined that 250°C is the optimal temperature for retrogression but in this study, since the main aim is to improve formability parameters as high as possible by keeping strength close to that of T6 level, formability parameters such as deformation hardening exponent (n) and anisotropy coefficient (R) were also be investigated.

Increasing amount of intermediate deformation has a decreasing effect on strain hardening exponent. Same tendency was observed for all sample orientations..

Retrogression temperature has a strong effect on strain hardening exponent. As the retrogression temperature increases, strain hardening exponent also increases accordingly. The highest strain hardening exponent values were obtained from the samples retrogressed at the highest retrogression temperature in this study (280°C).

Anisotropy coefficient is higher for the samples oriented 45° to the rolling direction than those oriented 0° and 90°. However, there is no apparent relationship between the anisotropy coefficient and retrogression temperature. On the other hand, anisotropy coefficient exhibited a decreasing trend with respect to the increasing intermediate deformation. It is more apparent that for the retrogression temperatures of 220° and 280°C.

RETROGRESYON VE YENİDEN YAŞLANDIRMA (RRA) UYGULANMIŞ 7075 ALAŞIMININ ŞEKİLLENDİRİLEBİLİRLİK PARAMETRELERİNE ARA DEFORMASYON İŞLEMİNİN ETKİSİ

ÖZET

Yüksek mukavemetli yaşlandırılmış 7xxx serisi Al-Zn-Mg-Cu alaşımları, zorlayıcı çalışma koşullarının etkin olduğu uçak yapılarında yaygın olarak kullanılmaktadır. Bu uygulamalar için dikkat edilmesi gereken önemli özellikler, dayanım, süneklik, korozyon direnci ve hasar toleransıdır (örneğin kırılma tokluğu ve yorulma dayanımı). 7075 alüminyum alaşımı 70 yıl önce geliştirilmiş olsa da son on yılda bu alaşım üzerine hala pek çok araştırma yapılmaktadır. 7xxx serisi alaşımlarda, ana alaşım elementi olarak çinko bulunmakla birlikte, önemli oranda bulunan diğer alaşım elementleri bakır ve magnezyumdur. Bu alaşımların mukavemeti, çökeltme sertleştirilmesi olarak tanımlanan ve T6 temper simgesi ile gösterilen bir ısıtılma işlemle artırılabilir.

T6 ısıtılma işlemi mekanik özellikleri geliştirmek için uygulanan ana ısıtılma işlemlerinden biridir ve bu kazanım, çözeltiye alma ve yaşlandırma aşamaları parametrelerinin optimizasyonu ile sağlanabilir. Dövme 7075-T6 Al alaşımı, 25 -100°C sıcaklık mükemmel mukavemete sahip çökeltmeyle sertleştirilmiş bir alaşımdır. Alaşımın çekme mukavemeti, 100°C üzerindeki sıcaklıklarda hızla düşmektedir.

RRA (Retrogresyon ve yeniden yaşlandırma) ısıtılma işlemi, T6 ısıtılma işlemine göre daha iyi mekanik mukavemet ve korozyon direnci sağlayan bir ısıtılma işlemidir. Bu durum literatürde önerilen sıcaklık aralığı (220 - 280°C) dışında kalan daha düşük bir aralığındaki (160 - 220°C) retrogresyon sıcaklıkları için de geçerlidir. RRA ısıtılma işlemi, T6 temper durumundaki bir alaşıma uygulanan iki kademeli bir ısıtılma işlemidir: Birinci aşama (retrogresyon aşaması) daha yüksek bir sıcaklıkta yapılır ve daha sonra alaşım T6 ısıtılma işlemindeki ile aynı koşulda yeniden yaşlandırılır (yeniden yaşlandırma aşaması).

7075 alaşımının RRA ısıtılma işleminin ilk aşamasında, malzeme solvus sıcaklığından daha düşük bir sıcaklığa tuz banyosu içinde ısıtılmakta ve sonra soğuk suda su verilmektedir. Bu aşama retrogresyon aşaması olarak adlandırılmaktadır. Malzeme

daha sonra yüksek mukavemet elde etmek için 120°C’de 24 saat süreyle yaşlandırılmaktadır.

Retrogresyon solvus sıcaklığı altında bir sıcaklık yapılsa da, bu sıcaklık GP zonlarının ve ince η' (MgZn_2) partiküllerinin çözünmesine yetecek kadar yüksek olmalıdır.

RRA ısıtıl işlemi sonrası elde edilen mikroyapı, tane içlerinde, T6 temper durumundakine benzer şekilde ince η' çökeltileri, tane sınırlarında ise T7 temper durumundakine benzer şekilde fine η çökeltilerinden oluşmaktadır. Bu mikroyapı bileşenleri dayanımda bir düşme yaratmaksızın korozyon direncini arttırabilir. Yüksek yoğunluktaki ince çökeltiler alaşıma mukavemet sağlarken, tane sınırlarındaki η partikülleri yüksek korozyon direnci sağlamaktadır.

Al-Zn-Mg-Cu (7xxx) alaşımlarının retrogresyon ısıtıl işlemi sırasında, tane içlerinde daha az kararlı olan mikroyapısal bileşenlerin (GP zonları ve daha ince η' çökeltileri) çözünmesi meydana gelirken, yeniden yaşlandırma, η' partiküllerinin tekrar çökmesini ve var olan partiküllerin ise büyüyerek η partiküllerine dönüşmesini sağlamaktadır. Bu bakımdan, retrogresyon ve yeniden yaşlandırma ısıtıl işlemi, tane içi ve tane sınırlarında bulunan partiküller arasındaki, boyut, mesafe ve dağılım farkını artmaktadır.

Bu çalışmada kullanılan malzeme ticari 7075-T6 (Al-Zn-Mg-Cu) alaşımıdır. Boyutları 2000 mm x 1000 mm x 2 mm (U x G x K) olan plaka şeklinde temin edilmiştir. Alaşıma üretim sonrası T6 ısıtıl işlemi uygulanmıştır. Ticari T6 ısıtıl işlemi prosedürü, 475°C sıcaklıkta 30 dakika süreyle çözeltiye alma ısıtıl işleminin ardından suda su verme ve ardından 120°C’de 24 saat süreyle yaşlandırma işleminden ibarettir. Çalışmada kullanılan çekme deneyi numuneleri, plakanın hadde yönüne 0°, 45° ve 90° açılarda çıkarılarak hazırlanmıştır.

Bu çalışmada, ara deformasyon işleminin RRA uygulanmış alaşımın, mukavemet ve şekillendirilebilirlik parametrelerine etkisini incelemek amacıyla, çekme deneyleri yapılarak, akma dayanımı, çekme dayanımı, çekme deformasyon sertleşmesi üssü (n değeri) ve anizotropi katsayısı (R değeri) belirlenmiştir.

Deneysel çalışma sonuçları, incelenen tüm oryantasyonlar için, RRA uygulanmış numunelerin akma ve çekme dayanımı ile sertliğinin T6 temper durumdaki alaşıma

göre düřtüđünü göstermektedir. Öte yandan, 250°C’de retrogresyon uygulanan numunenin, retrogresyon ve yeniden yařlandırma uygulanan numuneler içinde en yüksek akma ve çekme dayanımına sahip olduđu görülmüřtür. 220°C ve 280°C sıcaklıkrada retrogresyon uygulanan numunelerin akma ve çekme dayanımı deđerleri ise oldukça benzer olarak belirlenmiřtir. Yüksek mukavemet açısından, 250°C’nin optimum retrogresyon sıcaklıđı olduđu belirlenmiřtir. Ancak bu çalışmanın amacı, mukavemeti T6 seviyesine yakın bir deđerde korurken, řekillendirilebilirlik parametrelerini mümkün olduđu kadar iyileřtirmektir. Bu nedenle, deformasyon sertleřmesi üssü (n) ve anizotropi katsayısı (R) gibi řekillendirilebilirlik parametreleri de bu çalışmada incelenmiřtir.

Uygulanan ara deformasyon miktarının artmasının deformasyon sertleřmesini azaltıcı bir etkisi olduđu belirlenmiřtir. Bu davranıř, incelenen tüm numune oryantasyonlarında gözlenmiřtir. Retrogresyon sıcaklıđının deformasyon sertleřmesi üzerine önemli bir etkisi olduđu ve artan retrogresyon sıcaklıđı ile deformasyon sertleřmesi üssü deđerinin de arttıđı belirlenmiřtir. En yüksek deformasyon sertleřmesi üssü deđeri, bu çalışmada kullanılan en yüksek retrogresyon sıcaklıđında (280°C) elde edilmiřtir.

Anizotropi katsayısı, haddeleme yönüne 45° açıyla yönlenmiř numunede diđer oryantasyonlara (0° ve 90°) göre daha yüksektir. Ancak retrogresyon sıcaklıđı ile anizotropi katsayısı arasında belirgin bir iliřki belirlenmemiřtir. Diđer taraftan, anizotropi katsayısı, artan ara deformasyon miktarına bađlı olarak azalma eğilimi göstermektedir. Bu etki, 220°C ve 280°C retrogrsyon sıcaklıklarında daha belirgin olarak gözlenmiřtir.

1. INTRODUCTION

Research on new materials with low densities, high strengths, high stiffness, high fracture toughness, high thermal conductivities and low coefficients of thermal expansion for the applications to aerospace, automobile and electrical contact industries have been of tremendous interest to materials scientists [1]. The use of aluminum alloys in automotive industry has greatly increased in recent years. This has been attributed not only to the issues of fuel economy, but also to those of safety, resource conservation and environment friendliness [2].

High-strength age-hardened 7xxx series Al–Zn–Mg–Cu alloys are widely used for aircraft structures, where they are subjected to demanding operating conditions. Important properties that must be considered for these applications are strength, ductility, modulus, corrosion and damage tolerance (e.g. fracture toughness and fatigue resistance). Most of these properties can be controlled through appropriate alloying, processing or a combination of these [3].

7075 Aluminum alloy was developed over 70 years ago. However, many researches still have been performed on it in the past decade [4]. High strength and light weight properties of the alloy are attractive properties leading to its prevalent usage in transport applications corresponding to constantly increasing global warming concerns. In addition, 7075 Al alloy is being put into lightweight components of lower limb prostheses [5]. 7075 Aluminum alloy was commonly formed by wrought manufacturing process which resulted in high strength. However, the cost of this production route is very high compared to the alternative casting route. Nevertheless, disadvantages of conventional casting are found in the material structure with existence of casting defects such as pores and shrinkage cavities, including lower strength [6]. However, in order to obtain high strength 7075 Al alloy, heat treatment is a key process to improve mechanical properties after the forming process. T6 heat treatment is one of the major factors to enhance mechanical properties of the alloy through an optimization of both the solution heat treatment and the artificial aging conditions applied to the alloy [7,8]. T6 heat treatment schedule of wrought 7075 Al

alloy were well established at the solution temperature range of 465°– 490°C for 10 minutes and aging temperature of 120°C [9]. In contrast, dissolving soluble phases of the as-cast 7075 Al alloy should be done at temperature lower than 465°C as advised by Mukhopadhyay [10]. Moreover, various aging times at 120°C for 7075 Al alloy have been proposed to be the peak-aged condition of T6 heat treatment [11].

The T6-treated alloy has the highest strength, but poor stress corrosion resistance. By over-aging, the stress corrosion resistance can be improved, but the strength may be decreased by 10-15% [12]. For this reason, a lot of research on the mechanism of stress corrosion resistance and the improvement of heat treatment technology were carried out, thus the heat treatment regimes of T73, T74, T76 and T77 were developed successively. In order to obtain the strength of T6 and the corrosion resistance of T73 state, Cina [13] proposed a kind of three-step aging treatment, retrogression and re-aging (RRA) in 1974. The first and the third step aging treatments were equal to the T6 state peak aging treatment, and the second step aging treatment was retrogression at higher temperature. In order to adjust the quantity, size and distribution of the precipitates in the matrix and at grain boundaries, the retrogression time varied from 5 to 2400 s according to the retrogression temperature and the plate thickness [14]. However, most researches focused on the effects of retrogression temperature and retrogression time on the microstructures and mechanical properties [15].

During this investigation, with the aim of improving formability, strength and hardness of high strength 7075-T6 aluminum alloy, that is important in industry special in aerospace and aviation industry, retrogression and reaging (RRA) process and intermediate deformation was applied. During of this study effect of various retrogression temperature, changing step of intermediate deformation and different amount of hardening on formability, strength and hardness was investigated.

2. ALUMINUM AND ALUMINUM ALLOYS

2.1 History of Aluminum

Rare and expensive a century ago, aluminum has since been identified as the most common metal on earth, forming about eight percent of the earth's crust. It is the third most plentiful element known to man. Only oxygen and silicon (sand) exist in greater quantities. It was only in 1808 that Sir Humphrey Davy, the British electrochemist, established the existence of aluminum, and it was not until 17 years later that the Danish scientist Oersted produced the first tiny pellet of the metal.

The next step in the "discovery" of aluminum was the determination of its specific gravity by the German scientist Wöhler in 1845. He established one of aluminum's outstanding characteristics - lightness. He also discovered that it was easy to shape, was stable in air, and could be melted with a blow torch.

The production of primary aluminum is a young industry - just over 100 years old. But it has developed to the point where scores of companies in some 35 countries are smelting aluminum and thousands more are manufacturing the many end products to which aluminum is so well suited. For its first half century the aluminum industry pursued the dual role of improving and enlarging production processes to reduce the price of the metal and, at the same time, proving the worth and feasibility of aluminum in a wide range of markets. Such was the dynamic approach of the industry to this problem that the consumption of aluminum gained the remarkable record of doubling every ten years. The strong demand for aluminum stimulated the rapid expansion of productive capacity to meet it [16].

2.2 Physical Properties of Aluminum

2.2.1 Atomic structure of aluminum

Aluminum (or aluminium; see spelling differences) is a chemical element in the boron group with symbol Al and atomic number 13. It is a silvery white, soft, ductile metal. Aluminum is the third most abundant element (after oxygen and silicon), and

the most abundant metal in the Earth's crust. It makes up about 8% by weight of the Earth's solid surface (Figure 2.1) [17].

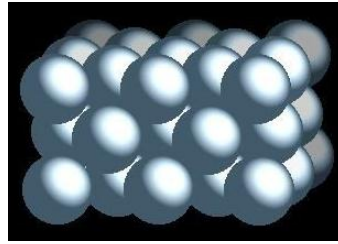


Figure 2.1 : Aluminum crystal structure [17].

2.2.2 Crystal structure

When metals change from the molten to the solid state, they assume crystalline structures. The atoms arrange themselves in definite ordered symmetrical patterns which metallurgists speak of as "lattice" structures. Aluminum, like copper, silver and gold, crystallizes with the face-centred-cubic arrangement of atoms, common to most of the ductile metals. This means that the atoms form the corners of a cube, with one atom in the centre of each face (Figure 2.2). The length of the sides of the cube for high purity aluminum has been determined as 4.049×10^{-8} cm. The face centred cubic structure is one of the arrangements assumed by close packed spheres, in this case with a diameter of 4.049×10^{-8} cm, the corners of the cube being at the centre of each sphere [16].

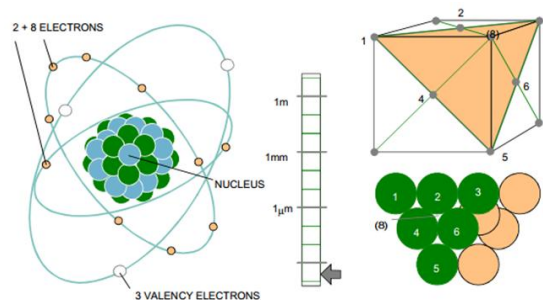


Figure 2.2 : Atomic structure of aluminum [16].

2.3 Classification of Aluminum Alloys

Each wrought aluminum alloy is designated by a four digit number. The first digit indicates the alloy group according to the major alloying element:

1xxx Aluminum 99.0% minimum;

2xxx Copper (1.9%...6.8%);

3xxx Manganese (0.3%...1.5%);

4xxx Silicon (3.6%...13.5%);

5xxx Magnesium (0.5%...5.5%);

6xxx Magnesium and Silicon (Mg 0.4%...1.5%, Si 0.2%...1.7%);

7xxx Zinc (1%...8.2%);

8xxx Others.

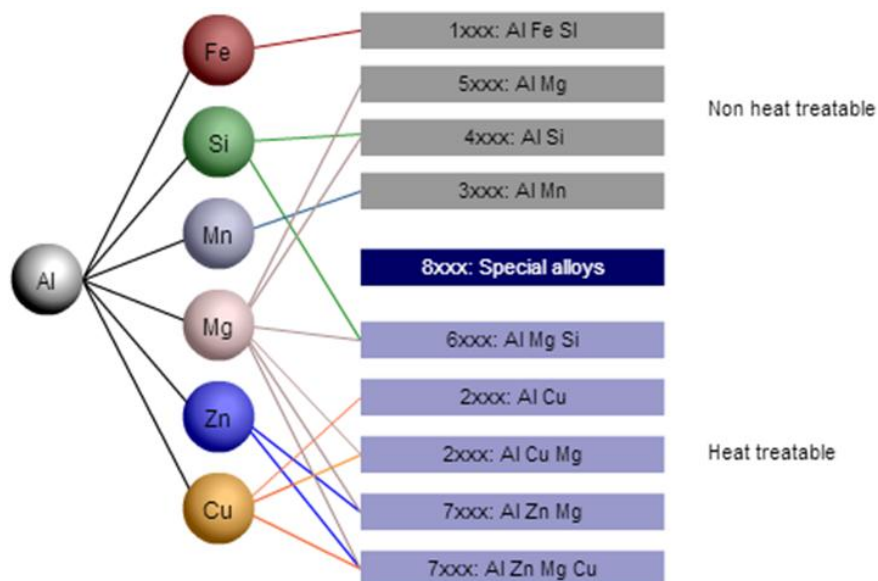


Figure 2.3 : Classification of aluminum alloys [18].

1xxx series alloys are pure aluminum and its variations; compositions of 99.0% or more aluminum are by definition in this series. Within the 1xxx series, the last two of the four digits in the designation indicate the minimum aluminum percentage. These digits are the same as the two digits to the right of the decimal point in the minimum aluminum percentage specified for the designation when expressed to the nearest

0.01%. As with the rest of the alloy series, the second digit indicates modifications in impurity limits or intentionally added elements. Compositions of the 1xxx series do not respond to any solution heat treatment but may be strengthened modestly by strain hardening [18].

2xxx series alloys have copper as their main alloying element, and because copper will go in significant amounts into solid solution in aluminum, these alloys will respond to solution heat treatment and are referred to as heat treatable [18].

3xxx series alloys are based on manganese and are strain hardenable. These alloys do not respond to solution heat treatment [18].

4xxx series alloys are based on silicon; some alloys are heat treatable, others are not, depending on the amount of silicon and the other alloying constituents [18].

5xxx series alloys are based on magnesium. They are strain hardenable, but not heat treatable [18].

6xxx series alloys have both magnesium and silicon as their main alloying elements, which combine as magnesium silicide (Mg_2Si) following solid solution. Alloys in this series are heat treatable [18].

7xxx series alloys have zinc as their main alloying element, often with significant amounts of copper and magnesium. They are heat treatable. 7xxx series are very strong “heat treatable” alloys; they can be strengthened through heat treatment (precipitation hardening) based on the combination of zinc (mostly between 4–6 wt.%) and magnesium (range 1–3 wt. %). Chromium amounts generally less than 0.35 % are added to increase the electrical resistivity. At higher content levels chromium tends to form very coarse constituents with other impurities or additions such as manganese, iron and titanium. Unfortunately these alloys seem prone to stress corrosion [18].

8xxx series contain one or more of several less frequently used major alloying elements such as iron or tin. The characteristics of this series depend on the major alloying element(s). Included in the 8xxx series are the relatively recently developed Al–Li alloys 8090, 8091 and 8093. Lithium has a significantly lower density than aluminum and since its solubility is also relatively high, it can be alloyed with aluminum in sufficient quantities to give a significant reduction in density (typically about 10% less than other aluminum alloys) [18].

As a major step towards alignment of Aluminum and Aluminum Alloy compositions on an international basis, most countries have agreed to adopt the 4 digit classification for wrought alloy composition designation. This system is administered by the Aluminum Association (AA), Washington USA, who compile the "Registration record of International Alloy Designations and Chemical Composition Limits for Wrought Aluminum Alloys". The European reference for the alloys will be identified with the preface EN and AW which indicated European Normative Aluminum Wrought alloys. In all other respects the alloy numbers and composition limits are identical to those registered by the Aluminum Association (Figure 2.4) [16].

Aluminium Alloy Designation System (CEN)						
		Major alloying element	Atoms in solution	Work hardening	Precipitation hardening	
WROUGHT ALLOYS*) EN AW-	1XXX	None (min. 99.00% Al)		X		Non-heat treatable alloys
	3XXX	Mn	X	X		
	4XXX	Si	X	X		
	5XXX	Mg	X	X		
	2XXX	Cu	X	(X)	X	Heat treatable alloys
	6XXX	Mg + Si	X	(X)	X	
	7XXX	Zn	X	(X)	X	
	8XXX	Other	X	(X)	X	
	9XXX0	Master Alloys				
	1XXX0	None (min. 99.00% Al)				

CASTING ALLOYS*) EN AB- EN AC- EN AM-	2XXX0 4XXX0 5XXX0 7XXX0 8XXX0 9XXX0	Cu Si Mg Zn Sn Master Alloys
--	--	---

*) letters preceding the alloy numbers have the following meaning
 EN = European Standard
 A = Aluminium
 B = Ingot
 C = Cast Alloy
 M = Master Alloy
 W = Wrought Alloy

Figure 2.4 : Aluminum alloy designation system [16].

2.3.1 Temper designations of non heat-treatable aluminum alloys

These are alloys in which the mechanical properties may be enhanced by the amount of cold work introduced after the last annealing operation. The properties so obtained will be reduced by subsequent heating and cannot be restored except by additional cold work [16].

In the non heat-treatable alloys there are generally six available tempers (Figure 2.5). It should be remembered, however, that all tempers are not always available for all alloys. The most common tempers range from annealed, designated by "0", to the full-hard tempers designated by temper HX8. The term H8 refers to the maximum

amount of cold work which is commercially practical for the particular alloy. An alloy in the HX8 condition will exhibit a 75% increase in strength over the same alloy in the "0" condition. Between the annealed and the HX8 state there are generally three intermediate levels of hardness referred to as:

Quarter hard	HX2
Half hard	HX4
Three quarters hard	HX6

Products are produced in the "F" temper, are defined as "as fabricated". "F" represents an undefined strength enhancement above the annealed state "0" [16].

H1, strain hardened only: Applies to products that have been strain hardened to obtain a desired level of strength without a supplementary thermal treatment. The number following H1 indicates degree of strain hardening.

H2, strain hardened and partially annealed: Applies to products that have been strain hardened more than the desired final amount, and their strength is reduced to the desired level by partial annealing. The number added to H2 indicates the degree of strain hardening remaining after partial annealing.

H3, strain hardened and stabilized: Applies to products that have been strain hardened and then stabilized either by a low temperature thermal treatment, or as a result of heat introduced during fabrication of the product. Stabilization usually improves ductility. The H3 temper is used only for those alloys that will gradually age soften at room temperature if they are not stabilized. The number added to H3 indicates the degree of strain hardening remaining after stabilization.

H4, strain hardened and lacquered or painted: Applies to products that are strain hardened and that have been subjected to heat during subsequent painting or lacquering operations. The number added to H4 indicates the amount of strain hardening left after painting or lacquering [18].

XXXX -F -O	as-fabricated annealed	
XXXX -H1 -H2 -H3 -HX2 -HX4 -HX6 -HX8	Work-hardened only Work-hardened and partially annealed Work-hardened and stabilized by low temperature treatment Quarter-hard Half-hard Three-quarter-hard Fully-hard	NON-HEAT TREATABLE ALLOYS
	Degree of cold working	
XXXX -T2 -T4 -T5 -T6 -T8	Cooled from an elevated temperature and naturally aged Solution heat-treated and naturally aged Cooled from an elevated temperature shaping process and artificially aged Solution heat treated and artificially aged Solution heat-treated, cold worked and aged	HEAT TREATABLE ALLOYS

Figure 2.5 : A Selection of common temper designations for aluminum alloys [16].

2.3.2 Temper designations of heat-treatable aluminum alloys

These are alloys in which the mechanical properties may be changed by heat treatment. Heat is used to enhance strength but can also be used to decrease strength through annealing to assist with forming; these alloys can also be re-heat-treated after annealing or forming to restore their original properties, This is a major difference compared with non heat-treatable alloys (Figure 2.5).The major tempers in this area are designated and defined according to international standards (AA, ISO, CEN):[16]

0 Fully annealed

T2 Cooled form an elevated temperature and naturally aged

T4 Solution heat-treated and naturally aged

T5 Cooled from an elevated temperature shaping process andthen artificially aged

T6 Solution heat-treated, artificially aged

T8 Solution heat-treated, cold worked and artificially aged

T2, cooled from an elevated temperature shaping process, cold worked, and naturally aged to a substantially stable condition: Applies to products (a) that are cold worked to improve strength after cooling from an elevated temperature shaping process or

(b) for which the effect of cold work in flattening or straightening is recognized in mechanical property limits

T4, solution heat treated and naturally aged to a substantially stable condition: Applies to products (a) that are not cold worked after solution heat treatment or (b) for which the effect of cold work in flattening or straightening may not be recognized in mechanical property limits

T5, cooled from an elevated temperature shaping process, then artificially aged: Applies to products (a) that are not cold worked after cooling from elevated temperature shaping process or (b) for which the effect of cold work in flattening or straightening may not be recognized in mechanical property limits

T6, solution treated, then artificially aged: Applies to products (a) that are not cold worked after solution treatment or (b) for which the effect of cold work in flattening or straightening may not be recognized in mechanical property limits

T7, solution heat treated and overaged/stabilized: Applies to (a) wrought products that are artificially aged after solution heat treating to increase their strength beyond the maximum value achievable to provide control of some significant property or characteristic or (b) cast products that are artificially aged after solution treatment to provide stability in dimensions and in strength.

T8, solution heat treated, cold worked, then artificially aged: Applies to products (a) that are cold worked to improve strength or (b) for which the effect of cold work in flattening and straightening is recognized in mechanical property limits [18].

In solution heat-treatment, the material is typically heated to temperatures of 900 to 1050 deg F, depending upon the alloy. This causes the alloying elements within the material to go into solid solution. Rapid quenching, usually in water, which freezes or traps the alloying elements in solution, follows this process [19].

The complete heat-treatment consists of a solution heat-treatment, a quenching process and subsequent aging, where the actual hardening occurs. It must be said that, unlike steel, aluminum alloys are definitely not hard after quenching [20].

Heat-treatable alloys are produced in many tempers. For structural engineering only a limited number is important and listed in Table 2.1. The wording "solution heat-treated" in Table 2.1 generally includes quenching. T5 is a special temper which does

not lie between T4 and T6 as most people would think. It is characterised by the fact that the material is not fully solution heat-treated (e.g. temperature too low) and also that the quenching may not be optimum. The result is lower strength values than T6 and lower values for elongation (poor formability). T6 characterises an artificially aging up to the maximum strength [20].

Table 2.1: The main tempers in use for structural application of precipitation hardened semi products [20].

Symbol	Description
T4	Solution heat-treated and then naturally aged
T5	Cooled from an elevated temperature shaping process and then artificially aged
T6	Solution heat-treated and then artificially aged
T61	Solution heat-treated and then artificially aged in underaging condition in order to improve formability (T65 between T61 and T6)
T66	Solution heat-treated and then artificially aged – mechanical property level higher than T6 achieved through special control of process 6000 series alloys
T7	Solution heat-treated and artificially over-aged
Tx51	These suffixes stand for a controlled stretching to relieve internal stresses coming from manufacturing (the fourth digit characterizes only variants – no influence on characteristic values)
Tx510	
Tx511	

2.4 Physical, Mechanical and Corrosion Properties of Aluminum Alloys

There are four basic ways in which aluminum can be strengthened: work hardening, dispersion hardening, solid solution hardening and precipitation hardening.

These hardening processes are effective because they produce conditions that impede the movement of dislocations. Dislocations are faults that enable metal crystals to slip at stresses very much below those that would be required to move two perfect crystal planes past one another [16].

2.4.1 Work hardening

Whenever aluminum products are fabricated by rolling, extruding, drawing, bending, etc., work is done on the metal. When work is done below the metal's recrystallisation temperature (cold work), it not only forms the metal, but also increases its strength due to the fact that dislocations trying to glide on different slip planes interact causing a "traffic jam" that prevents them from moving. Fabricating processes carried out above the metal's recrystallization temperature (hot work) do

not normally increase strength over the annealed strength condition. With non heat-treatable wrought alloys, cold work is the only way of increasing strength. With heat treatable alloy, cold work applied after heat treating can increase strength still further. Work hardening of non heat treatable aluminum magnesium and pure aluminum alloy is shown in Figure 2.6 [16]

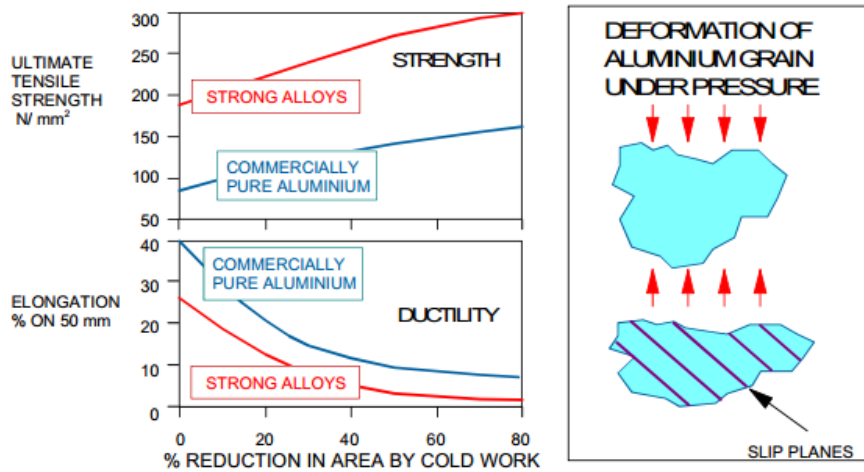


Figure 2.6 : Work hardening of aluminum [16].

2.4.2 Dispersion hardening

-Fine particles of an insoluble material are uniformly distributed throughout the cristal lattice in such a way as to impede the movement of dislocations (eg 3000 series). With aluminum, dispersion-hardening may be achieved in two ways:

- by the addition of alloying elements that combine chemically with the metal or each other to form fine particles that precipitate from the matrix
- by mixing particles of a suitable substance (for example A1 203) with powdered aluminum and then compacting the mixture into a solid mass.

2.4.3 Solid solution hardening

Most alloys are solid solutions of one or more metals dissolved in another metal: either the alloying of atoms take over the lattice positions of some of the base-metal atoms (substitutional solid solutions) or they occupy spaces in the lattice between the base-metal (interstitial solid solutions). In both cases, the base-metal lattice is distorted, retarding the movement of dislocations and hence strengthening the metal. The 5000 series with magnesium as the solute is a good example.

Most aluminum alloys reflect some solid solution hardening as a result of one or more elements being dissolved in the aluminum base, each element's contribution to the strength of the alloy is roughly additive. Usually these alloys are further strengthened by heat treatment or by work hardening [16].

2.4.4 Precipitation hardening

Precipitation hardening is a two stage heat treatment. It can be applied only to those groups of alloys which are heat treatable (i.e. 2000, 6000 and 7000 wrought series). Firstly, a supersaturated condition is produced by solution heat treatment. Secondly the "aging" process that occurs after quenching may be accelerated by heating the alloy until a second and coherent phase is precipitated. This coherent phase strengthens the alloys by obstructing the movements of dislocations. Solution treatment involves heating the alloy to a temperature just below the lowest melting point of the alloy system, holding at this temperature until the base metal dissolves a significant amount of the alloying elements (Figure 2.7).

The alloy is then rapidly cooled to retain as much of the alloying elements in solution as possible and so produce a supersaturated solid solution. This supersaturated condition is usually unstable and therefore heat-treatable alloys are used in this condition, i.e. T4 [16].

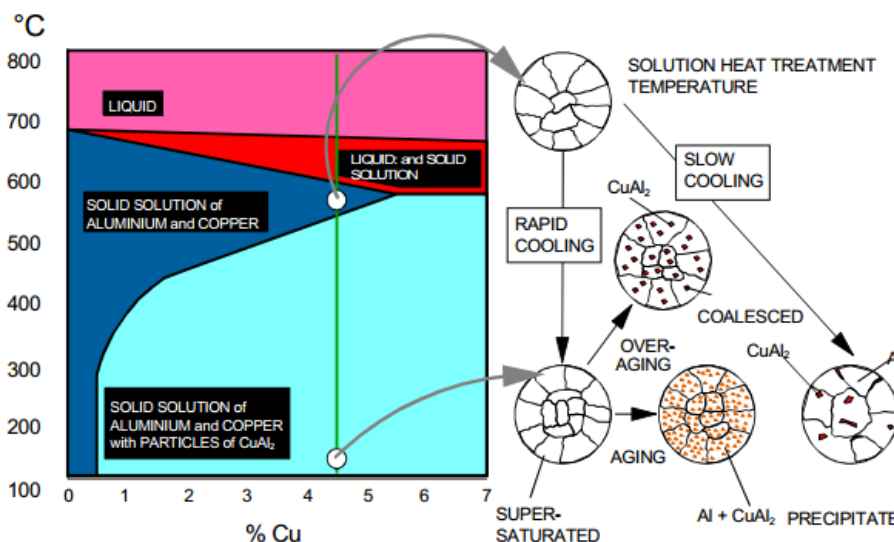


Figure 2.7 : Metallurgy of precipitation hardening (e.g Al -Cu system) [16].

2.4.5 Electrical conductivity and resistivity of aluminum

The electrical conductivity of 99.99% pure aluminum at 200°C is 63.8% of the International Annealed Copper Standard (IACS). Because of its low specific gravity, the mass electrical conductivity of pure aluminum is more than twice that of annealed copper and greater than that of any other metal.

The resistivity at 200°C is 2.69 microhm.cm. The electrical conductivity which is the reciprocal of resistivity, is one of the more sensitive properties of aluminum being affected by both, changes in composition and thermal treatment. The addition of other metals in aluminum alloys lowers the electrical conductivity of the aluminum therefore this must be offset against any additional benefits which may be gained, such as an increase in strength. Heat treatment also affects the conductivity since elements in solid solution produce greater resistance than undissolved constituents [16].

2.4.6 Tensile strength

The natural qualities of aluminum and its alloys are positive deciding factors for designers, manufacturers and industrial users who are always on the lookout for better-performing materials and innovative processes [21].

Behavior under tension is generally considered the first yardstick of an engineering material, and Figure 2.8 shows typical tensile stress/strain curves for four different aluminum alloys and compares them with a range of engineering metals. The alloys are: 99.5% pure aluminum (1050A) in the fully annealed state, suitable for deep pressing; a 4.5% magnesium-aluminum alloy (5083) after strain-hardening, by rolling, to the "half-hard" temper, used in marine and welded structures; a magnesium-manganese-silicon alloy 6082 after solution treatment and aging to the fully heat treated "T6"-condition, used in commercial structures and a zinc-magnesium-copper-aluminum alloy 7075 in the fully heat treated condition used in aircraft construction [16].

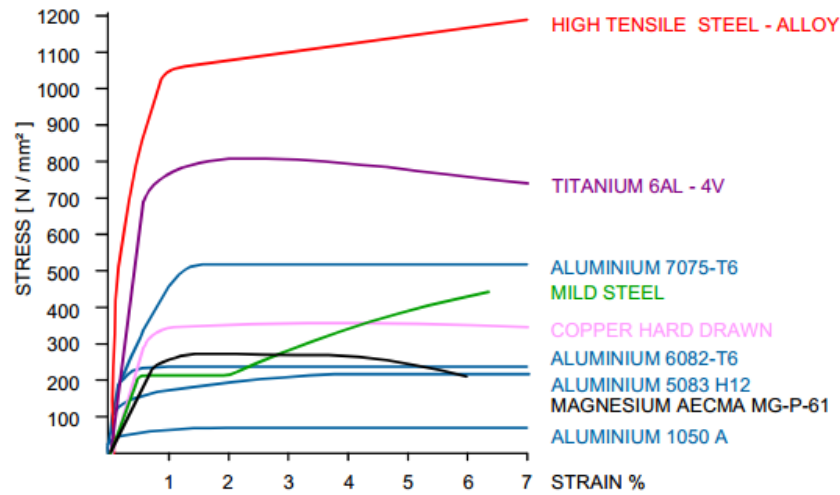


Figure 2.8 : Stress-strain curves of aluminum in comparison with various metals and alloys [16].

2.4.7 Proof Stress

With mild steel there is a clearly defined point on the stress strain curve at which the elastic limit is reached; this "yield point" is followed by a sharp reduction in the stress before the metal exhibits a plastic flow region with stress again increasing with strain until the ultimate stress is reached and the stress reduces to the point of failure. In most cases no clearly defined elastic limit or yield point is to be seen on stress/strain curves for aluminum alloys, this is apparent by looking at Figure 2.9. For this reason the point of departure from the elastic range has to be defined arbitrarily. For convenience in routine testing, a point is chosen at which the permanent deformation is easily measured: at one time, a permanent set of 0.1% of the original gauge length was used. Today, however, 0.2% is the international norm [22].

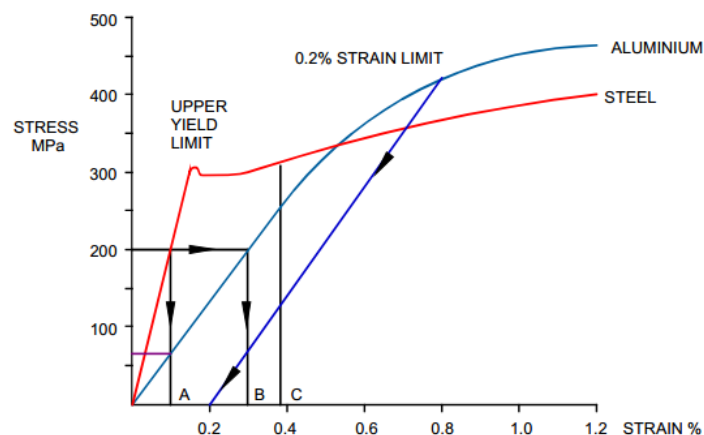


Figure 2.9 : Plastic yield behavior of aluminum and mild steel [22].

If we compare the curves for a similar strength aluminum and steel (Figure 2.9) and consider a 0.1% strain by drawing a vertical line at A the stress in the steel is 200 MPa whereas in the aluminum is only 66.6 MPa. It can also be seen from the graph that a strain of 0.3% (line B) is necessary to induce the same stress in the aluminum member. It is also worth noting that the aluminum represented by the curve in Figure 2.8 would still be in the elastic range at 0.38% strain (line C) while the steel subjected to the same rate of strain would have entered the plastic range [16].

2.4.8 Elastic Properties

From Figure 2.9 it can be seen that for the initial part of the stress-strain curve the strain per unit increase of stress is much higher for aluminum than for steel, measurement shows that it is three times higher. The slope of this part of the curve determines the Modulus of Elasticity (Young's Modulus) e.g. stress divided by strain. It follows therefore that the Modulus of Elasticity for aluminum is one-third that of steel, being between 65500 and 72400 MPa for most aluminum alloys. From the information already given it is clear that when a steel structural member is replaced by one of identical form in an aluminum alloy the weight will be one third but the elastic deflection will be about three times as large. From this we can deduce that an aluminum member of identical dimension to one in steel will absorb three times as much energy, but only up to the point where the stress in the aluminum remains below the limit of proportionality [16].

2.4.9 Hardness

Resistance to surface indentation is an approximate guide to the condition of an alloy, and is used as an inspection measure. (steel ball), Vickers (diamond) and Shore Scleroscope (diamond Hammer) testing machines are applied to aluminum alloys; typical Brinell values range from 20 for annealed commercially pure-metal to 175 for the strongest alloy. Hardness readings should never be regarded as a quantitative index to tensile strength, as is often done with steels, for in aluminum the relation between these two properties is far from constant. The surface hardness of aluminum can be increased considerably by the process of hard anodising (500VPN) and is therefore often employed to improve the wear resistance of components [16].

2.4.10 Corrosion Resistance

Aluminum has a higher resistance to corrosion than many other metals owing to the protection conferred by the thin but tenacious film of oxide. This oxide layer is always present on the surface of aluminum in oxygen atmospheres. The graph (Figure 2.10) shows the degree of corrosion and its effect on strength in two different environments. The famous statue of Eros in London's Piccadilly Circus is an example of the corrosion resistance; after an inspection following eighty years of exposure to the London atmosphere, the statue showed only surface corrosion. The formation of the oxide is so rapid in the presence of oxygen that special measures have to be taken in thermal joining processes to prevent the oxide instantly forming while the process is being carried out [16]

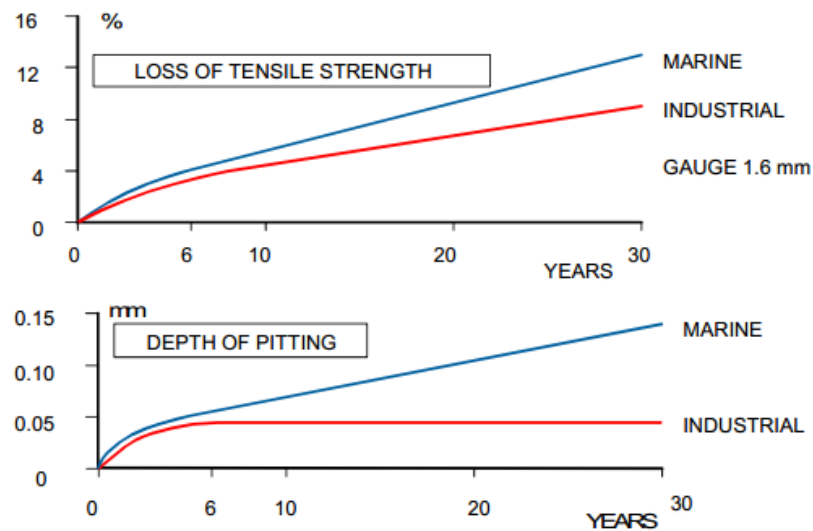


Figure 2.10 : Pitting corrosion behavior of 3103 mill finish aluminum sheet [16].

2.5 Comparison of Aluminum Alloys

Figures 2.11 - 2.14 show the relationship between the properties and characteristics of the various alloy groupings. For instance, natural, unalloyed aluminum possesses an ultimate tensile strength of about 70 MPa which compares to 700 MPa and above for some of the 7XXX series [16].

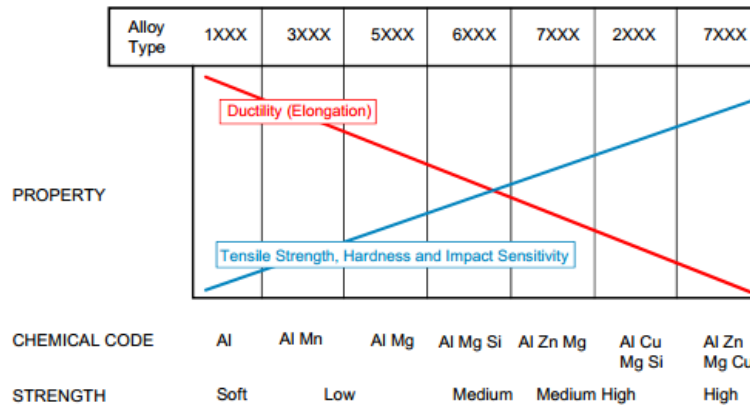


Figure 2.11 : The effect of alloying elements on tensile strength, hardness, impact Sensitivity and Ductility [16].

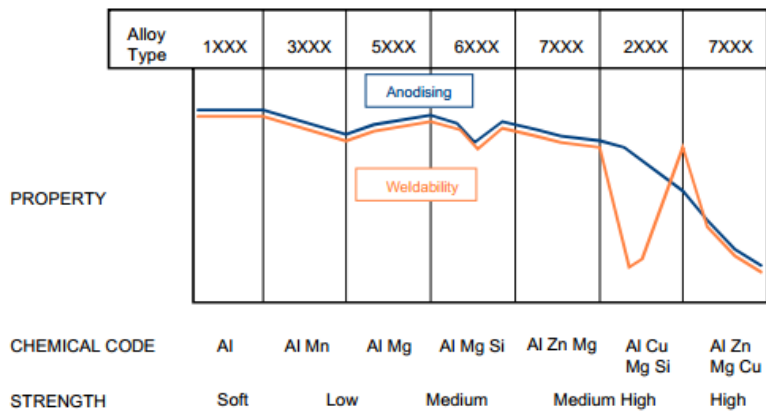


Figure 2.12 : The effect of alloying elements on weldability and anodising [16].

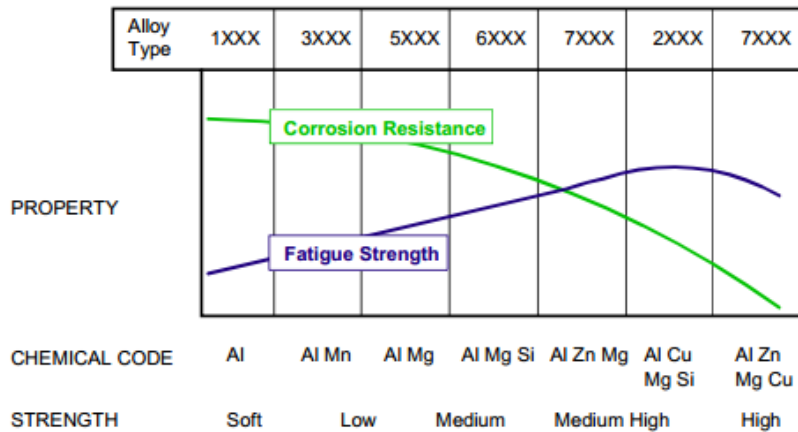


Figure 2.13 : The effects of alloying elements on corrosion resistance and fatigue strength [16].

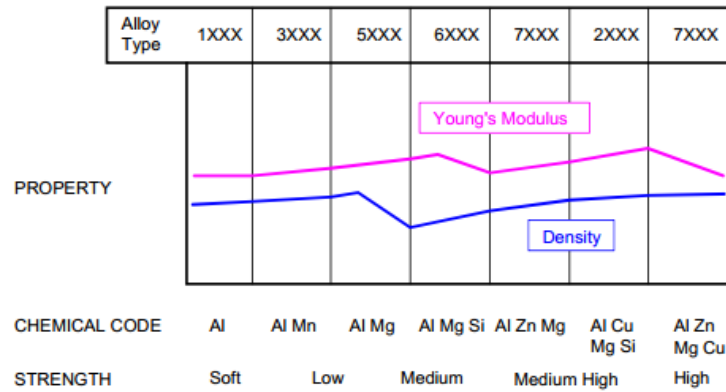


Figure 2.14 : The effect of alloying elements on density and young's modulus [16].

2.6 7075 Aluminum Alloy

The first 7075 was developed in secret by a Japanese company, Sumitomo Metal, in 1936. 7075 was used for the Mitsubishi A6M Zero fighter's air frame for the Imperial Japanese Navy starting in 1940.

High strength and light weight properties of the alloy are attractive properties leading to its prevalent usage in transport applications corresponding to constantly increasing global warming concerns. In addition, 7075 Al alloy is being put into lightweight components of lower limb prostheses [11].

7075 Aluminum alloy was commonly formed by wrought manufacturing process which resulted in high strength. However, the cost of this production route is very high compared to the alternative casting route. Nevertheless, disadvantages of conventional casting are found in the material structure with existence of casting defects such as pores and shrinkage cavities, including lower strength. An alternative Semi-Solid Metal (SSM) process was developed in early 1971. Reduction in casting temperature and solidification shrinkage is its main advantage. This SSM process has since been developed into thixocasting and rheocasting processes[11].

Aluminum alloy 7075 is an aluminum alloy, with zinc as the primary alloying element. It is strong, with a strength comparable to many steels, and has good fatigue strength and average machinability, but has less resistance to corrosion than many other Al alloys. Its relatively high cost limits its use to applications where cheaper alloys are not suitable [16].

7075 aluminum alloy shows strongly brittle fracture under high-speed penetration test even at room temperature, small fracture surfaces of another kind on the bottom of shallow-stretched dimples were also observed. This characteristic brittle fracture of A7075 is due to the fracture of the chemical compound of Mg and Zn in A7075 [23].

7075 aluminum alloy's composition roughly includes 5.6–6.1% Zn, 2.1–2.5% Mg, 1.2–1.6% Cu, and less than half a percent of Si, Fe, Mn, T, Cr and other metals. It is produced in many tempers, some of which are 7075-0, 7075-T6, 7075-T651.

Among the various classes of high strength aluminum alloys, the 7xxx series (Al–Zn–Mg–Cu alloy system) possesses higher strength and has been widely used in heavy-duty applications such as aerospace industry. The deformation behavior of the 7xxx series aluminum alloys at high temperatures has been carried out extensively [24].

Table 2.2 Comparison of mechanical properties for T0 and T6 tempers [24].

Alloy	Temper	Proof Stress 0-2% (MPa)	Tensile Strength (MPa)	Shear Strength (MPa)	Elongation A5 (%)	Hardness Vickers (HV)
AA7075	T0	105-145	222-275	150	9	65
	T6	435-505	510-570	130	5	160

Wrought 7075-T6 Al alloy is a precipitation-hardened alloy that possesses excellent mechanical properties at temperatures between 25 and 100°C. Its tensile strength sharply decreases with increasing temperature at temperatures above 100°C, however. For example, the tensile strength of commercial 7075- T651 Al alloy decreases from 598 MPa at 25°C to 297 MPa at 200°C [25]. Three types of intermetallics were observed in AA7075-T6 (Figure 2.14): $\text{Al}_7\text{Cu}_2\text{Fe}$, $(\text{Al,Cu})_6(\text{Fe,Cu})$ and Mg_2Si . $\text{Al}_7\text{Cu}_2\text{Fe}$ intermetallic had a size of 1 – 20 μm and were characterized by a higher Cu content than $(\text{Al,Cu})_6(\text{Fe,Cu})$ intermetallics [26].

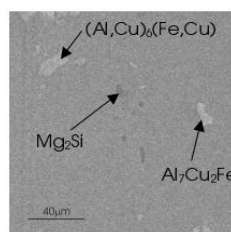


Figure 2.15 SEM micrograph of AA7075-T6 alloy [26].

The heat treatment that has been deemed optimal for the 7075 alloy is the T6 temper [7]. 7075 Aluminum solution heat treated at 475°C for 30 min and quenched in water, then artificially aged at 120°C for 24 h to create the T6 temper [27]. At all the solution treatment temperatures, water quenched samples always had higher hardness values [7]. Its tensile strength sharply decreases with increasing temperature at temperatures above 100°C. Microstructure stability enhanced creep resistance of 7075 Al alloy has been achieved by addition of Zr, which forms small precipitates of Al₃Zr as a stable dispersoid phase [25].

In order to obtain high strength 7075 Al alloy, heat treatment is a key process to improve mechanical properties after the forming process. T6 heat treatment is one of the major factors to enhance mechanical properties of the alloy through an optimization of both the solution heat treatment and the artificial aging conditions applied to the alloy [28]. T6 heat treatment schedule of wrought 7075 Al alloy were well established at the solution temperature range of 465–490°C and aging temperature of 120°C [9]. In contrast, dissolving soluble phases of the as-cast 7075 Al alloy should be done at temperature lower than 465°C as advised by Mukhopadhyay [10]. Moreover, various aging times at 120°C for 7075 Al alloy have been proposed to be the peak-aged condition of T6 heat treatment [11].

The peak strength is developed through the T6 condition, while the T7 produces superior corrosion resistance. In general, these temper specific properties are controlled by the precipitation sequence [29]:

Solid solution → Guinier Preston (GP) zones → η' → η equilibrium phase

G-P zones are metastable, coherent solute clusters of Zn, Mg and Cu. The metastable η , MgZn₂ or more correctly Mg(ZnCuAl)₂ appear as discrete platelet particles that are semi coherent with the matrix, which is known to populate within the grains, and η is pseudostable, non-coherent of the same phase appearing as rods or plates, which is known to populate the grain boundary [30]. T6 heat treatment data of the 7075 Al alloy produced by rheocasting process along with a GISS technique. This is focused into two main sections of T6 heat treatment; solution heat treatment and artificial aging. The influence of solution heat treatment and artificial aging temperature and time on mechanical properties and microstructures was investigated [11].

2.6.1 Effect of age hardening on microstructure and mechanical properties of 7075-T6 Aluminum alloys

Aging treatment was carried out in order to increase the strength and hardness of the alloy. During a proper solution treatment, the alloy constituents would be dissolved as much as possible without forming brittle and coarse particles. If the alloy is rapidly cooled, e.g., by quenching in water, this rich solid solution will not be stable and excess elements or compounds would precipitate out of the solution resulting in an increase in strength of the alloy. The aging temperatures used in this study were 120°C, 145°C, 165°C, and 185°C. Figure 2.16 shows how the hardness of the specimens varies as a function of time at each aging temperature [11].

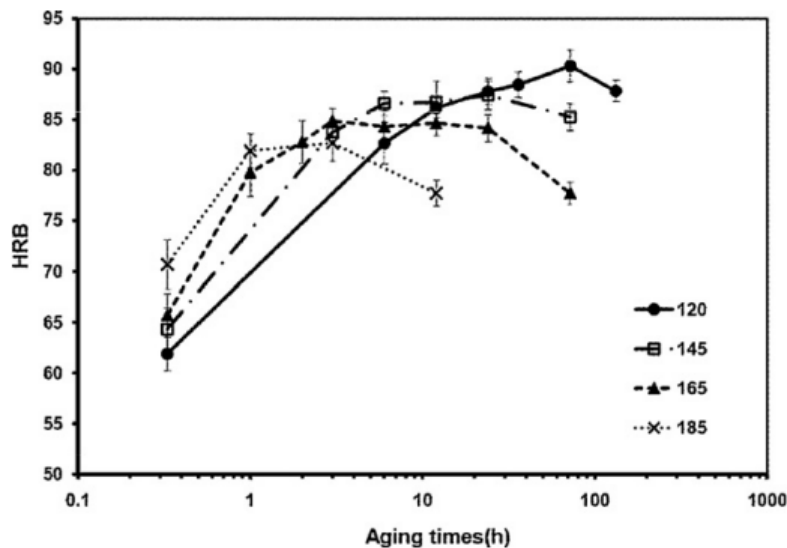


Figure 2.16 : Hardness vs. time for various aging temperatures [11].

The tensile strength and % elongation of the alloy aging to the peak hardness value and the onset hardness plateau values are shown in Figure 2.17.

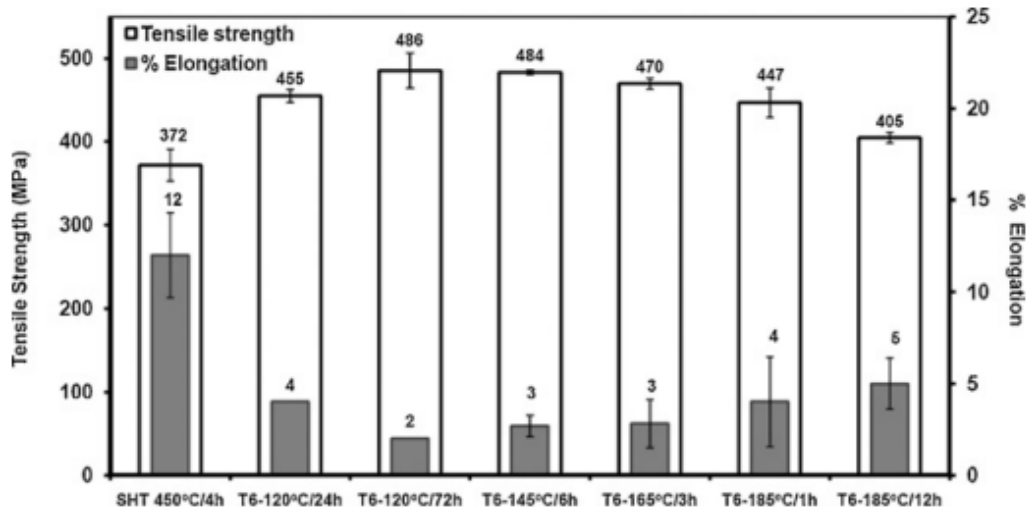


Figure 2.17 : Tensile strength and % elongation of GISS-processed rheocasting 7075 Al alloy after T6 aging process at various temperatures and time durations [11].

Figure 2.18 shows the difference in precipitate size and number density of specimens aged at various conditions. High density of very fine GP zone was observed in the specimen aged at an underaged condition of 120°C for 24 h as shown in Figure 2.18a.

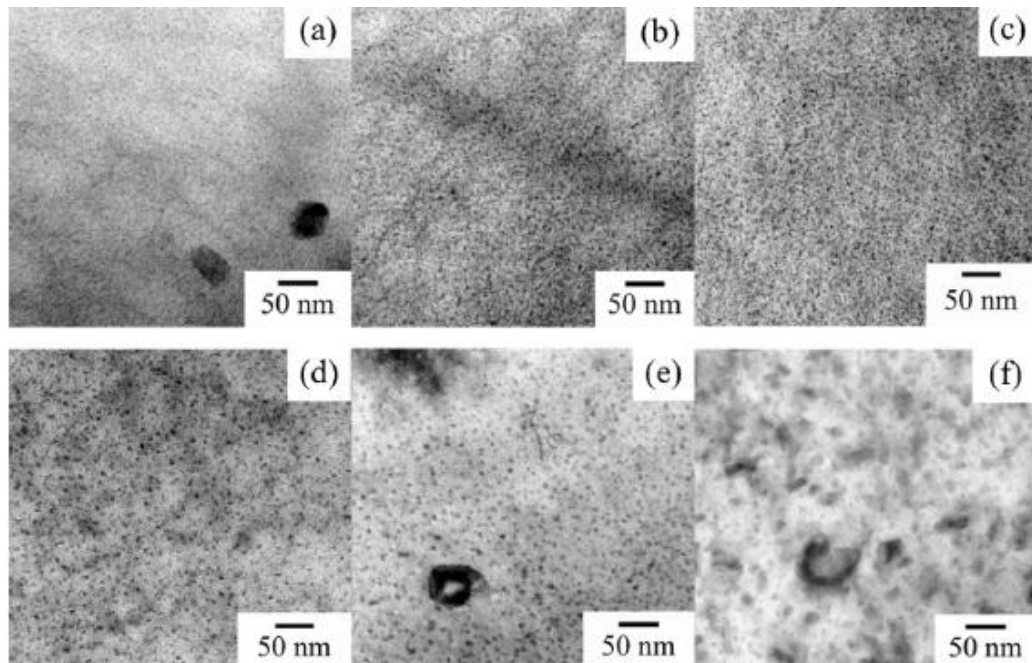


Figure 2.18 : TEM bright field imaging in [0 1 1] zone axis of specimen aged at (a) 120°C for 24 h; and in [1 1 4] zone axis of specimens aged at (b) 120°C for 72 h (c) 145°C for 6 h (d) 165°C for 3 h (e) 185°C for 1 h and (f) 185°C for 12h [11].

3. RETROGRESSION AND REAGING (RRA) HEAT TREATMENT

3.1 Introduction

Age-hardenable alloys that are peak aged to the T6 or T8 temper possess the highest strength. For the 7xxx series aluminum alloys, when they are peak aged, they are highly susceptible to stress corrosion cracking (SCC) which can lead to premature failure. One way to remedy this problem is to over age the material to a T7 temper but this causes the aluminum alloy to lose 10-17% of its strength. A solution to this problem is retrogression and reaging (RRA) [31].

RRA are capable of producing a material with mechanical and stress corrosion strengths higher than those presented by the T6 temper; this remaining true even for a lower range of retrogression temperatures (from 160° to 220°C) than that recommended in the literature (220°-280°C). Mechanical and stress corrosion cracking strength obtained after the RRA were higher than those characteristic of the T6 temper [32,33]. RRA consist of applying to the alloy in the T6 temper a double stage thermal cycle: the first stage (retrogression) runs at higher temperature and is followed by a stage similar to that used to obtain the T6 temper (re-aging) [34]. The duration of the first higher temperature stage is the necessary for the maximum solution of the T6 precipitates to occur; a minimum mechanical strength is being associated with this temper. During the second lower temperature stage (the reaging treatment) the solute re-precipitates and the mechanical strength increases again [35].

3.2 Process

The heat treatment process of RRA involves a material being heated to a high temperature just below the solvus line for a short period of time in a salt bath and after that, sample quenching in cold water. This step of the process is called retrogression. The material is then reaged for 24 hours at 120°C to back to its peak strength to provide high strength and SCC resistance. It was reported that

retrogression is essentially a grain boundary precipitate coarsening treatment [36]. Figure 3.1 schematically shows of RRA heat treatment.

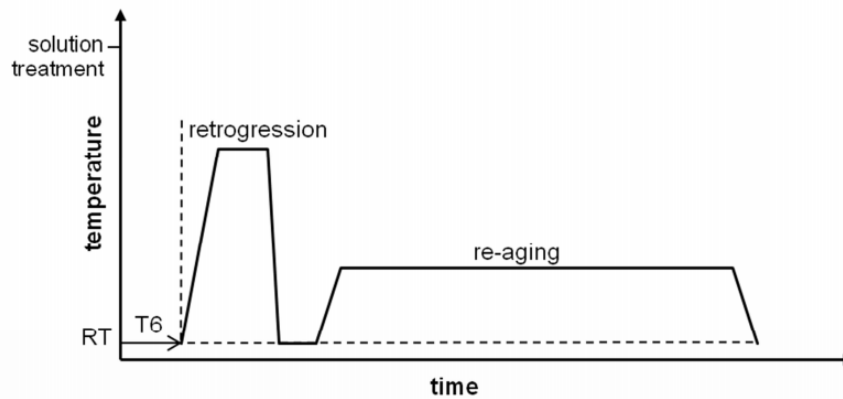


Figure 3.1 : Thermal cycle diagram of the two-step retrogression and reaging treatment after T6 temper [37].

3.3 Effect of RRA on microstructure

The high mechanical strength developed by the alloy in the T6 temper is associated with a high density metastable precipitation, distributed homogeneously in the aluminum matrix; whilst a lower density of thicker precipitates, more stable in nature, is the microstructure responsible for the inferior strength of the overaged T7 temper. Whilst maintaining the T6 temper microstructure inside the grains, RRA treatments promote coarsening of grain boundary precipitation; this microstructure becomes similar to that of the T7 temper; the overall microstructure being more stable in nature than that for the T6 temper [38].

The high density of fine precipitates is responsible for the high mechanical strength achieved with these treatments. The stress corrosion resistance of the alloy is generally thought to be controlled by the microstructure near to grain boundaries (the size and spacing of precipitates, free precipitation zones, and solute concentration gradients): the effect of these parameters is however not fully understood, but it is well known that the susceptibility of these alloys to stress corrosion cracking decreases with aging time [39,40].

Commercial purity aluminum alloys contain numerous constituent particles that have electrochemical potentials different from that of the matrix and corrosion pits can readily develop at these particles. Once corrosion pits are formed they act as stress

concentration sites leading to stress corrosion cracking [41]. In commercial aluminum alloys, pitting corrosion has been found to occur at intermetallic constituent particles. According to Gao et al. [42], two types of particles were identified.

Type A particles were anodic with respect to the matrix and tend to dissolve themselves, while type C particles were cathodic to the matrix and tended to promote dissolution of the adjacent matrix. Types A particles were those with Al, Mg, and Zn and type C particles were those with Fe, Cu, Mn. The conventional method of solving the low corrosion resistance problem has been to overage the material (T73). Consequently a strength loss of 10–15% was inevitable. Retrogression and reaging was advised in order to overcome this problem. This method consists of retrogression the T6 structure at a high temperature within the two-phase field, then reaging at the original T6 condition [3].

Retrogression should be carried out at a temperature below the solvus line of the alloy, but high enough to allow for the partial or complete dissolution of GP zones and fine η' (MgZn_2) precipitates [43]. The microstructure resulting from the RRA is fine η' precipitates within the grains similar to the T6 condition and η precipitates distribution at the grain boundaries similar to the T7 temper. The microstructure characterization can improve corrosion resistance without strength loss [43]. In the retrogression stage, this dissolution results from the combination of the growth of the large (stable) precipitates and the dissolution of the smaller (unstable) ones [44]. During retrogression, the hardness and yield strength of alloy 7075 decreases rapidly as the Guinier-Preston (GP) zones dissolve. Stage 2 is a transient recovery period where the hardness increases as the remaining η' grows to a near optimum size and distribution. The hardness reaches a maximum and then begins to decrease as this η' coarsen excessively and starts transforming to η [45].

For Al–Zn–Mg–Cu (7xxx) alloys, retrogression is responsible for the dissolution of the less stable precipitates (GP zones and the finer particles of η') inside the grains, and re-aging promotes the re-precipitation of θ whilst its pre-existent particles grow and transform to η [46]. Hence a retrogression and re-aging process can increase the difference of size, spacing and distribution between grain and grain boundary precipitates. It can also coarsen precipitates on the grain boundaries and

increase their dispersion [47]. The main precipitation sequence of Al–Zn–Mg–Cu alloys can be summarized as follows:

supersaturated solid solution (SSS) \longrightarrow GP (Zn, Mg) zones \longrightarrow Meta-stable η' Stable η (MgZn_2), and the main strengthening precipitates are the GP zones and η' phases [48].

In the peak aged (T6) treatment, the main precipitates inside the grains are fine and homogeneously distributed precipitations η' . After the alloy was retrogressed, the main changes of the microstructure are the dissolution of the meta-stable η' phase inside the grains. While re-aging promotes a dense re-precipitation of η' inside the grains and the grain boundary equilibrium precipitates continue the growth process initiating during retrogression [47]. Hence inside the grains, the RRA microstructure is similar to that for T6 treatment, but is slightly denser and coarser and more stable in nature. Contrarily, the equilibrium phases on the grain boundaries coarsen obviously, distributing discontinuously and isolated [49].

If the retrogression treatment is continued later than the end of its dissolution stage, a coarsening stage occurs rapidly, where precipitates are observed to grow to large sizes and volume fraction increases [50]. To get the largest fraction of fine precipitates inside the grain, it was suggested that retrogression should be carried out in the range of 170–260°C, while re-aging should be at 120 °C [26,51]. Retrogression is responsible for the dissolution of the less stable precipitates (GP zones and the finer particles of η') inside the grains, and re-aging promotes the re-precipitation of η' whilst its pre-existent particles grow and transform to η [52]. Retrogression and re-aging process can increase the difference of size, spacing and distribution between grain and grain boundary precipitates. It can also coarsen precipitates on the grain boundaries and increase their dispersion [53]. Figure 3.2 shows the TEM bright field micrographs within the grain of the 7075 Al alloy with the T6, T73 and RRA treatments. The precipitates of η' with fine size and high density are observed within the grain of the alloy with the T6 and RRA treatments (Figures 3.2a and b). This microstructural feature is consistent with their high strength [18].

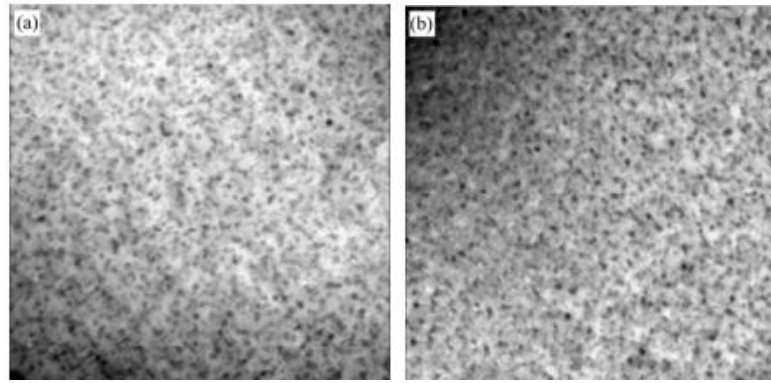


Figure 3.2 : TEM bright field micrographs within grain for (a) 7075-T6 alloy and (b) 7075-RRA alloy [18].

The stress corrosion resistance of the alloy is generally thought to be controlled by the microstructure near to grain boundaries (the size and spacing of precipitates, free precipitation zones, and solute concentration gradients): the effect of these parameters is however not fully understood, but it is well known that the susceptibility of these alloys to stress corrosion cracking decreases with aging time [38].

In the T6 temper the TEM micrographs reveal a very fine precipitation distributed homogeneously inside the grains with coarser and less space at grain boundary precipitates, as can be seen in Figure 3.3 [38].

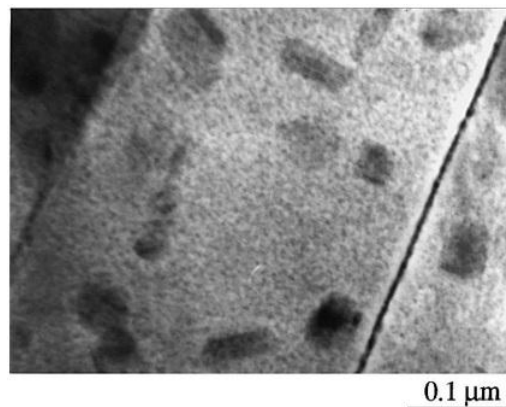


Figure 3.3 TEM microstructure of the T6 temper [38].

The precipitation inside the grains after retrogression is similar to that of the T6 temper, whilst the grain boundaries show very coarse precipitate as well apart, very similar to the T7 temper grain boundary precipitation, as presented in Figure 3.4; these observations leading to the conclusion that the grain boundary precipitates have followed a coarsening process [38].

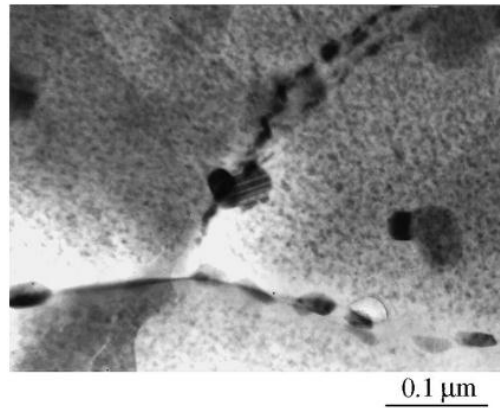


Figure 3.4 TEM microstructure after retrogression at 200°C [38].

Reaging promotes a very dense precipitation inside the grains whilst the grain boundary precipitates continue the growth process initiated during retrogression (Figure 3.5). No effect of retrogression temperature was detected. The RRA microstructure is similar to that for the T6 temper, but is a little coarser and denser inside the grains: contrarily, the grain boundary precipitation is quite different, and very similar to that of the overaged T7 temper [38].

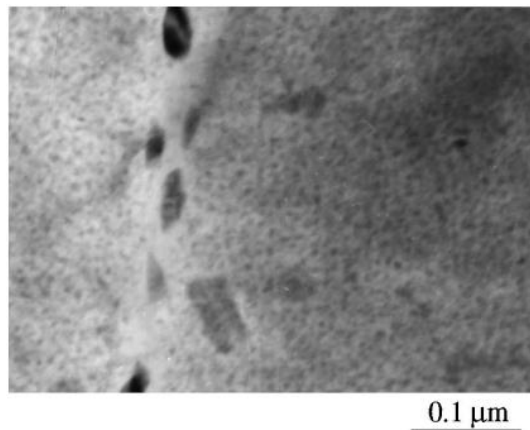


Figure 3.5 TEM microstructure after RRA (retrogression at 180°C) [38].

3.3.1 Effect of RRA on fractograph

Figure 3.6 shows the fractographs of the alloy after T6 and RRA heat treatment, respectively. It is demonstrated that the fractures of two conditions are all in transgranularl/intergranular combined mode. And both conditions represent fibrous ductile fiacture, with many small dimples inside the surface of fibrous fracture. There are more transcrystalline fractures, and fewer intergranular fractures caused by the second phases within the dimples. The fracture behavior of alloy is due to the

reduction of undissolved coarser phase and the increase of precipitated phase (the increase of yield strength) [26].

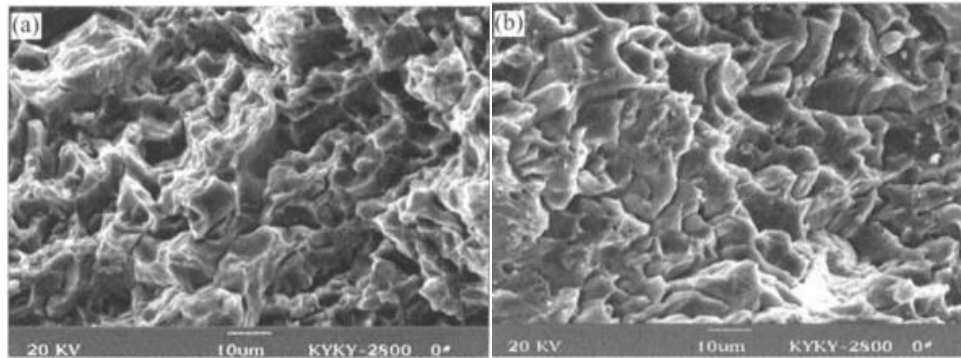


Figure 3.6 SEM fractographs of alloy after (a) T6 and (b) RRA treatments [26].

3.3.2 Effect of retrogression time on microstructure

Retrogression and the RRA treatment with different retrogression times are shown in Figure 3.7. The precipitates of small size decrease obviously in the retrogression sample for 7 min, which indicates that the GP zones and η' phase of small size are redissolved in a relatively short time. After retrogression for 45 min, there is a noticeable increase in precipitates size [54]. After retrogression at 200°C for 7 min and then re-aging under the same condition as the pre-aging (100°C for 24 h), the volume fraction of η' and η precipitates increases over both the original pre-aging condition and the corresponding retrogressed condition (the minimum in the retrogression curve). The grain boundary precipitates mainly consist of stable particles such as η . With the extension of retrogression time, the size of precipitate in the matrix is gradually coarsened (Figure 4.6d and e) as well as the η precipitates on the grain boundoury [26].

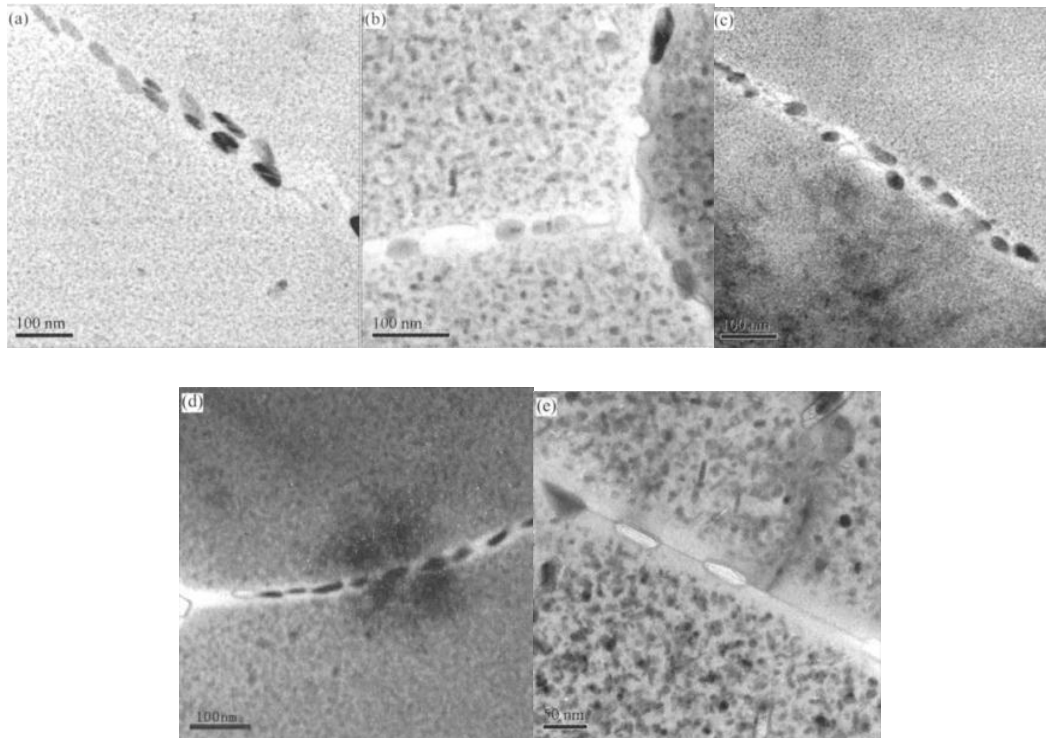


Figure 3.7 : Microstructural evaluation of the alloys after retrogression and RRA
 (a) Retrogression at 200°C for 7 min., (b) retrogression at 200°C for 45 min., (c) Retrogression at 200°C for 7 min. and reaging, (d) retrogression at 200°C for 17 min. and reaging, (e) retrogression at 200°C for 45 min. and reaging [26].

4.EXPERIMENTAL PROCEDURE

In this study effect of RRA heat treatment and intermediate deformation on the strength, formability and hardness of high strength aluminum alloy (7075-T6) has been investigated.

4.1 Material

The material used in this study is a commercial 7075-T6 aluminum alloy (Al–Zn–Mg–Cu alloy). It was received in the form of sheet with the dimensions of 2000 mm x 1000 mm x 2 mm (l x w x t). The alloy has been given T6 temper. Commercial heat treatment procedure for T6 temper is solution treatment at 475°C for 30 min., quenched in water, and then artificially aged at 120°C for 24 h. The chemical composition of the studied 7075-T6 aluminum alloy is shown in Table 4.1. Tensile test samples were cut from the plate in different orientations such as 0°, 45° and 90° to the rolling direction.

Table 4.1 : Chemical composition of the studied 7075-T6 alloy (in wt. %).

Zn	Mg	Cu	Cr	Fe	Si	Ti	Mn	Al
5.75	2.59	1.53	0.19	0.14	0.07	0.05	0.02	Balance

4.2 Retrogression and Reaging Heat Treatment

In this process, salt bath furnace was used for heating the samples to the retrogression temperature. This furnace can increase the temperature of samples in a short time. In this process, three retrogression temperatures such as 220°C, 250°C and 280°C were used and the samples were retrogressed at those temperatures for 1 min. After that, the samples taking out of furnace and quenched in cold water of 5-8°C temperature. Subsequently intermediate deformations were applied to the samples in 2%, 4% and 6% and one sample was left undeformed for comparison. Furthermore, one sample was deformed 2% after reaged. Following intermediate

deformations, the samples were reaged at 120°C for 24 and then cooled to room temperature in air.

In this study, the samples were divided into 3 groups with respect to their rolling directions of 0°, 45° and 90° degrees and 5 identical samples were tested or each rolling direction. Therefore 15 samples were tested for each retrogression temperature. Table 4.2 shows experimental layout.

Table 4.2 : Experimental layout for intermediate deformation.

Temperature	Rolling orientation	Intermediate Deformation
220° C / 250° C / 280°C	0°	0%
		2% After retrogression
		4% After retrogression
		6% After retrogression
		2% After reaging
	45°	0%
		2% After retrogression
		4% After retrogression
		6% After retrogression
		2% After reaging
	90°	0%
		2% After retrogression
		4% After retrogression
		6% After retrogression
		2% After reaging

4.3 Intermediate Deformations and Tensile Tests

Tensile test specimens were prepared according to ASTM-E8M standards. Intermediate deformation and tensile tests were carried out on a hydraulic controlled 100 kN Shimadzu testing machine. Cross head speeds during all mechanical tests were 0.5 mm.s⁻¹ and strain was measured by a 50 mm gage length axial extensometer attached to the gage section of the samples.

By performing tensile tests, 0.2% yield strength, ultimate tensile strength, elongation at fracture, tensile strain hardening exponent (*n*) and anisotropy coefficient (*R*) were determined. In order to determine strain hardening exponent ASTM E646 standard

was followed and anisotropy coefficient was calculated by measuring the width strain by a micrometer with an accuracy of 0.01 mm. Anisotropy coefficient values were calculated for an axial strain of 10%. Equations to calculate anisotropy coefficient were given in Eqs. 4.1 to 4.4.

$$\text{Longitudinal strain } \varepsilon_l = \ln \frac{l_i}{l_o} \quad (4.1)$$

where l_i : the instantaneous length of the sample and

l_o : original gage length

$$\text{Transverse strain } \varepsilon_w = \ln \frac{w_i}{w_o} \quad (4.2)$$

where w_i : the instantaneous width of the sample and

w_o : original width

During uniform plastic deformation, volume is constant, so the thickness strain can be calculated as

$$\text{Thickness strain } \varepsilon_t = 0 - \varepsilon_l - \varepsilon_w \quad (4.3)$$

Assuming that

$$\varepsilon_l + \varepsilon_w + \varepsilon_t = 0$$

Therefore, anisotropy coefficient (R) can be calculated as

$$R = \frac{\varepsilon_w}{\varepsilon_t} \quad (4.4)$$

Following anisotropy coefficients for each sample orientation, average anisotropy coefficient (normal anisotropy coefficient, $R_{ave.}$) and planar anisotropy coefficients (ΔR) were also calculated by Eqs. 4.5 and 4.6.

$$R_{ave.} = \frac{R_0 + R_{90} + 2R_{45}}{4} \quad (4.5)$$

$$\Delta R = \frac{R_0 + R_{90} - 2R_{45}}{2} \quad (4.6)$$

The value of R_{ave} , higher than unity is an indicator that the sheet has a resistance against thinning during forming. This reduces thinning and neck formation in the sheet at the highly stressed locations during deep drawing and hence enhances draw ability. ΔR is desirable for resistance against earing. If the amount of this factor is being near to zero, high resistance of the sample against earing is obtained.

The tensile strain hardening exponent n is defined as the slope of logarithm of true stress and true strain curve. This equation can be written as follows:

$$\sigma_t = K.\varepsilon^n \quad (4.7)$$

This equation can be transformed into a logarithmic one as follows:

$$\log \sigma_t = \log K + n \log \varepsilon \quad (4.8)$$

The strain hardening exponent in the logarithmic system of coordinates is defined as the slope of the corresponding straight line.

4.4 Hardness Tests

Hardness of the samples was measured by a Vickers indenter (a diamond pyramid) with a load 10 kg on a Zwick ZHU 2.5 hardness tester. At least five measurements were taken for each sample and the results were averaged.

4.5 Electrical Conductivity Measurements

In order to investigate effects of retrogression temperature and intermediate deformation on electrical conductivity, electrical conductivity of all samples was measured by AutoSigma 3000 equipment operating at 60 kHz according to eddy current principle. Three measurements were made on each sample in the unit of mS/m (mega-Siemens/meter) and the results were averaged. Electrical conductivity measurements in the unit of mS/m can be converted into %IACS unit (International Annealed Copper Standard) through Eq. 4.7:

$$\% IACS = \frac{mS/m}{58} \times 100 \quad (4.7)$$

% IACS unit is based on the annealed pure copper the electrical conductivity in a system as 100%.

5. EXPERIMENTAL RESULTS AND DISCUSSION

5.1 Tensile Tests

By performing tensile tests, yield strength, ultimate tensile strength, elongation at fracture, tensile strain hardening exponent and anisotropy coefficient were calculated. In the following sections, effect of retrogression temperature, intermediate deformation amount and sample orientation were given.

5.1.1 Result of ultimate tensile strength, yield strength and elongation

Figures 5.1 to 5.2 show variation of yield strength, ultimate tensile strength (UTS), yield and elongation at fracture for different retrogression temperatures and sample orientations.

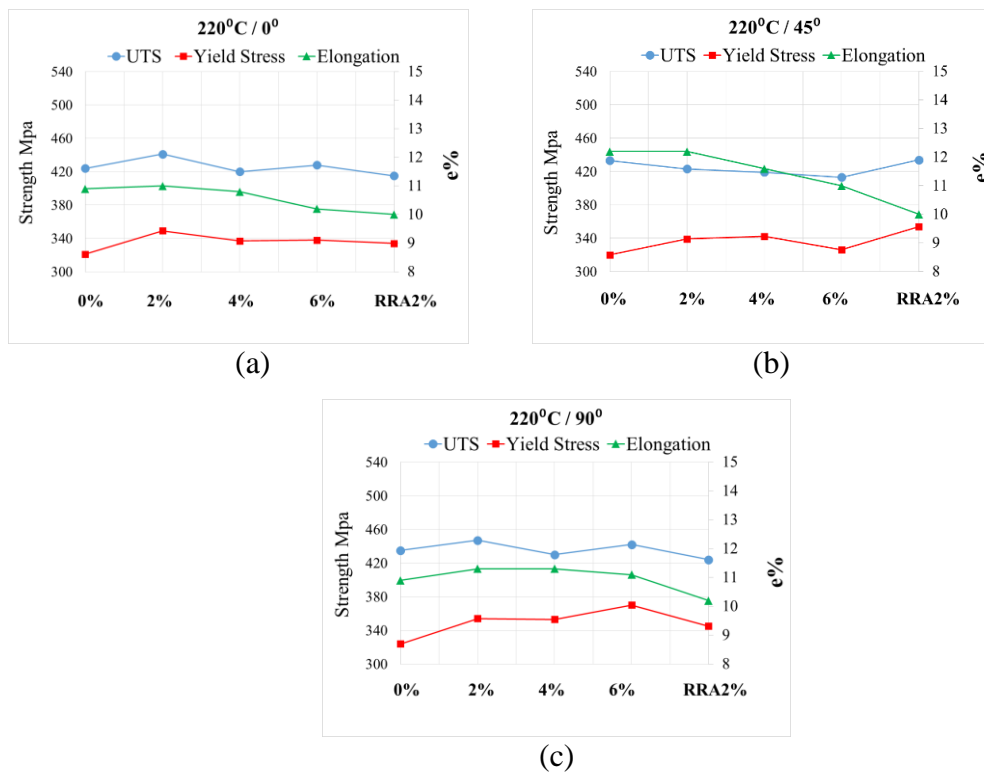
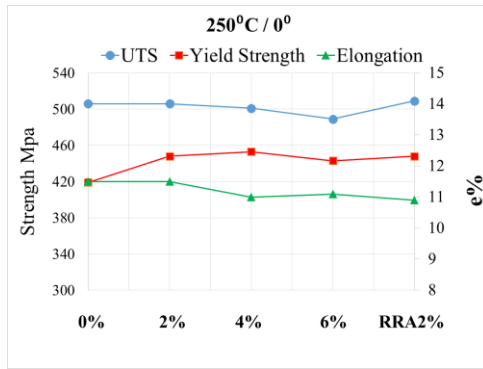
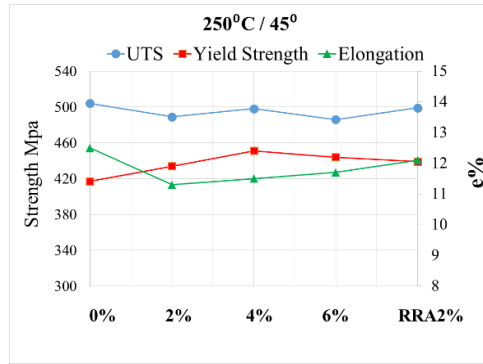


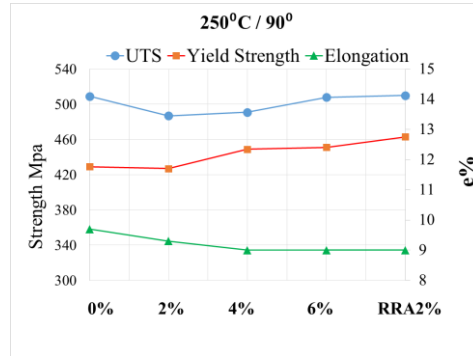
Figure 5.1 : Variation of strength and elongation at fracture of the samples retrogressed at 220°C and then reaged as a function of intermediate deformation for different orientations.



(a)

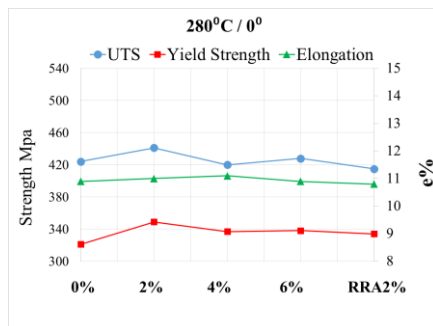


(b)

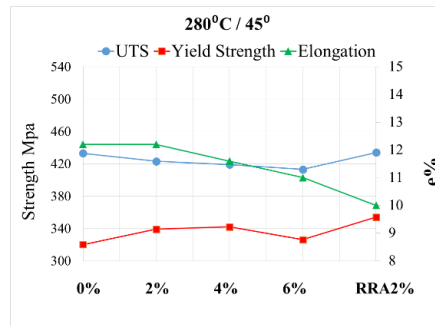


(c)

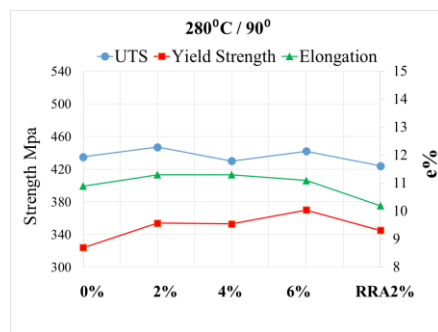
Figure 5.2 : Variation of strength and elongation at fracture of the samples retrogressed at 250°C and then reaged as a function of intermediate deformation for different orientations.



(a)



(b)



(c)

Figure 5.3 : Variation of strength and elongation at fracture of the samples retrogressed at 280°C and then reaged as a function of intermediate deformation for different orientations.

Figures 5.1 to 5.3 indicate that rolling orientation does not have any clear effect on UTS and yield strength in all temperatures, but we can observe the effect of this factor on the elongation but this effect is not very significant. With comparing diagrams it is determined that the amount of elongation at 45° is higher than 0° and 90° and, value of elongation at 0° and 90° are close to each other.

Figures 5.4 to 5.6 show variation of yield strength, ultimate tensile strength and elongation at fracture with respect to retrogression temperature. They apparently show that for all rolling orientations, retrogression temperature of 250°C has the highest UTS and yield strength, while 220°C and 280°C have nearly similar UTS and yield strength. For obtaining high strength, it is determined that 250°C is the optimal temperature for retrogression but in this study, aim is not only high strength, but also increasing formability of alloy with increasing strength or keeping strength as high as possible, is the main goal, therefore amount of n and R should also be taken into account. Figures 5.6 shows variation of elongation at fracture for retrogression temperatures of 220°C, 250°C and 280°C, respectively. It is clear that elongation at fracture values for the retrogression temperature of 250°C are higher than the others.

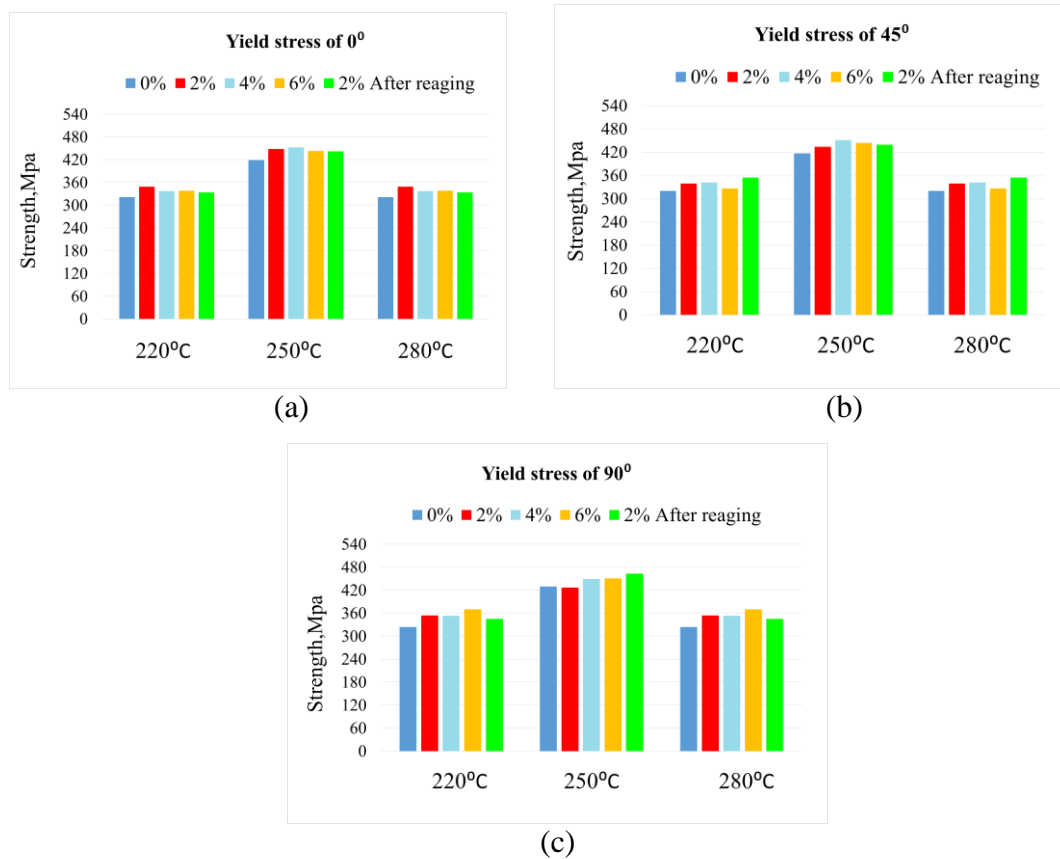


Figure 5.4 : Variation of yield strength as a function of retrogression temperature for different intermediate deformations and orientations.

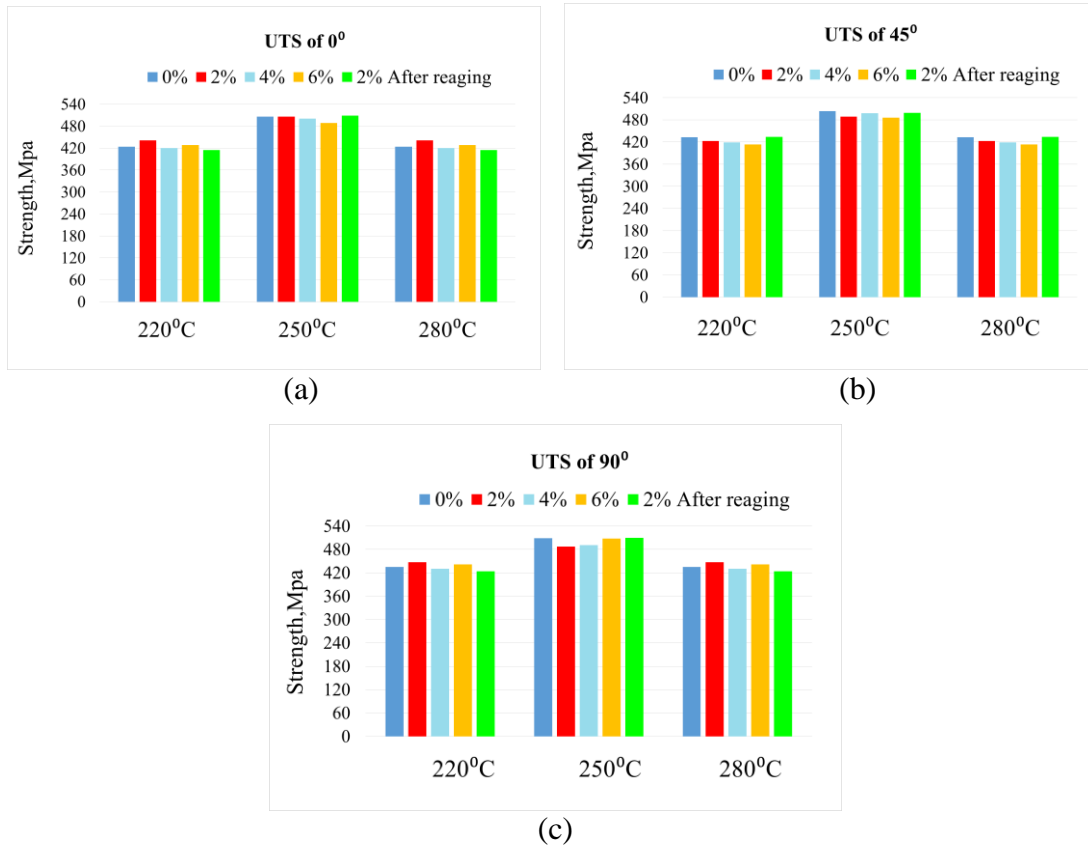


Figure 5.5 : Variation of ultimate tensile strength as a function of retrogression temperature for different intermediate deformations and orientations.

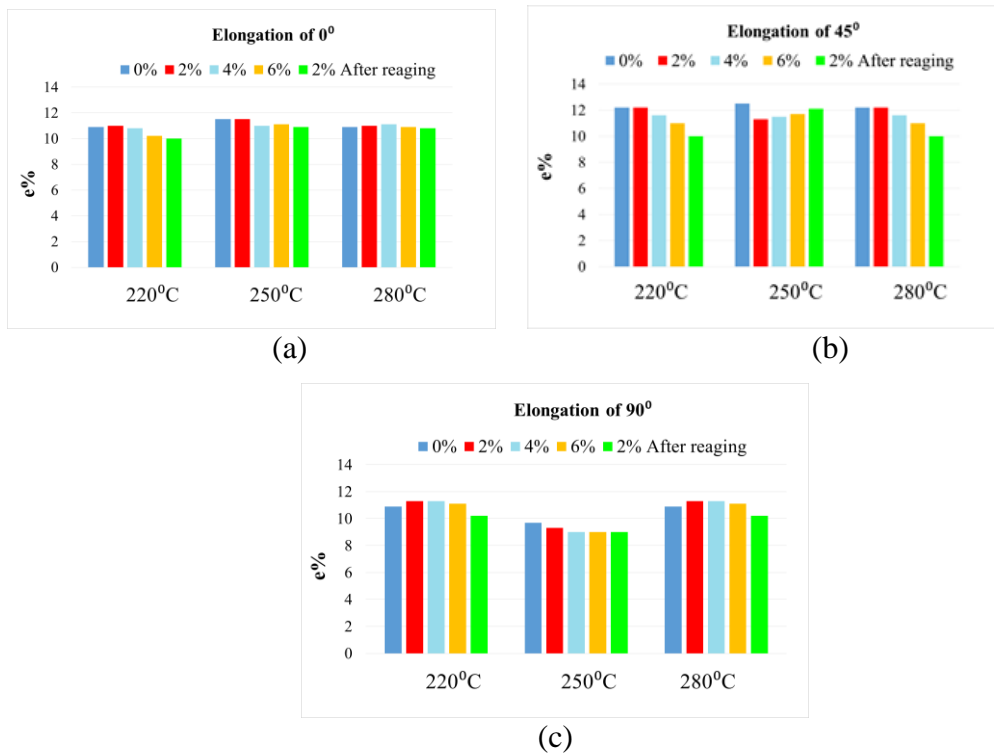


Figure 5.6 : Variation of elongation at fracture as a function of retrogression temperature for different intermediate deformations and orientations.

5.1.2 Result of strain hardening exponent (n)

5.1.2.1 Effect of intermediate deformation

Figure 5.7 shows variation of strain hardening exponent with respect to intermediate deformation for different retrogression temperatures. It is clear that increasing amount of intermediate deformation has a decreasing effect on strain hardening exponent. Same tendency was observed for all sample orientations. Also, increasing retrogression temperature increases strain hardening exponent. As already mentioned, amount of n is usually lies between 0 and 1, and with increasing amounts of n formability increases. It suggests that increasing overaging is beneficial for strain hardening exponent. On the other hand, 2% deformation after reaging slightly increases strain hardening exponent for all samples except those oriented 90° to the rolling direction.

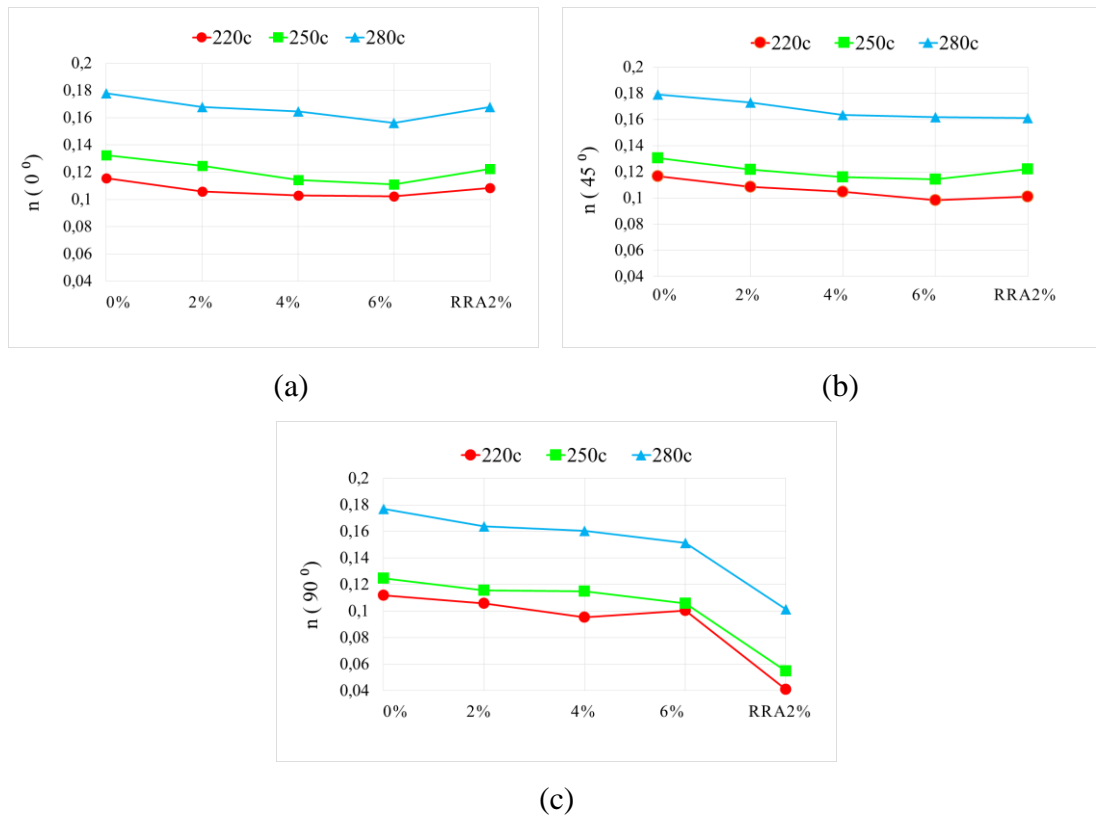


Figure 5.7 : Variation of strain hardening exponent as a function of intermediate deformations at different retrogression temperatures for the sample orientations of (a) 0° , (b) 45° and (c) 90° .

Figure 5.8 shows variation of strain hardening exponent with respect to intermediate deformation for different sample orientations for different retrogression temperatures. There is no clear relationship between strain hardening exponent and sample orientation for the studied retrogression time interval. It should be mention that 2% deformation after reaging decreases strain hardening exponet for the sample oriented 90° to the rolling direction. This effect is clear for all retrogression temperatures.

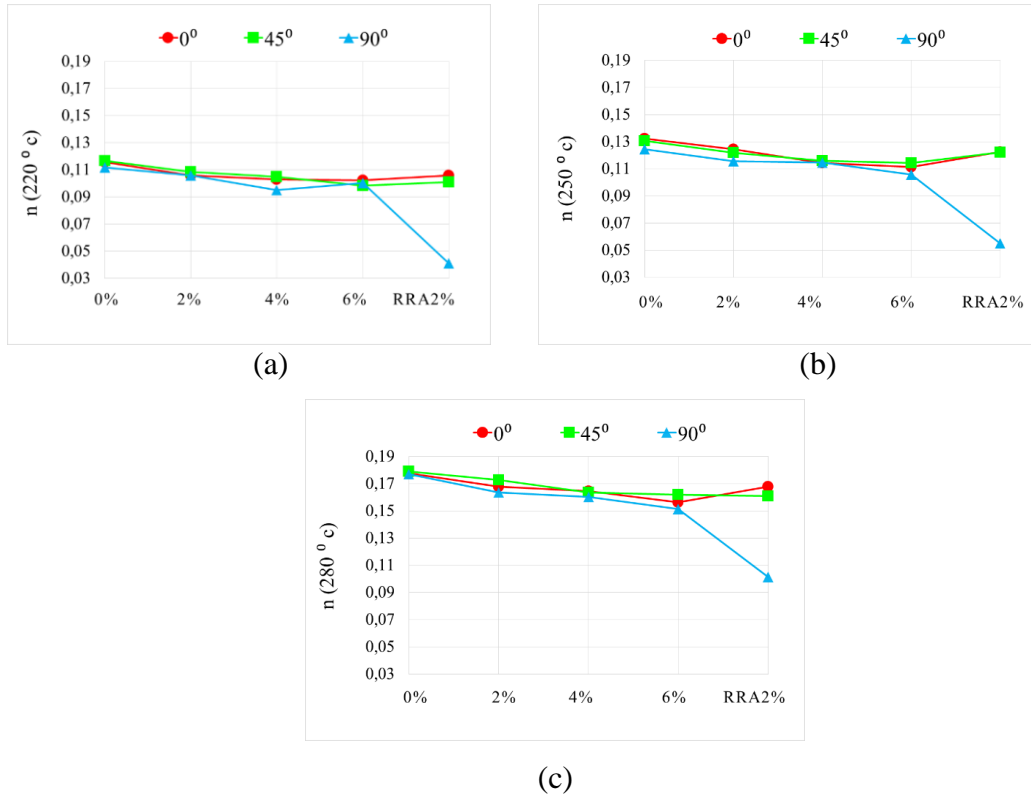


Figure 5.8 : Variation of strain hardening exponent as a function of intermediate deformations for different sample orientations for the samples retrogressed at (a) 220°C, (b) 250°C and (c) 280°C.

5.1.2.2 Effect of rolling orientation

Figure 5.9 shows variation of strain hardening exponent with respect to sample orientation. It should be first noted that here is no clear effect of sample orientation on strain hardening exponent. However, as shown from Fig. 5.9 a to c, as the retrogression temperature increases, strain hardening exponent increases. It should also be noted that samples oriented at 90° to the rolling direction have a decreasing effect on strain hardening exponent when the sample was deformed 2% after reaging.

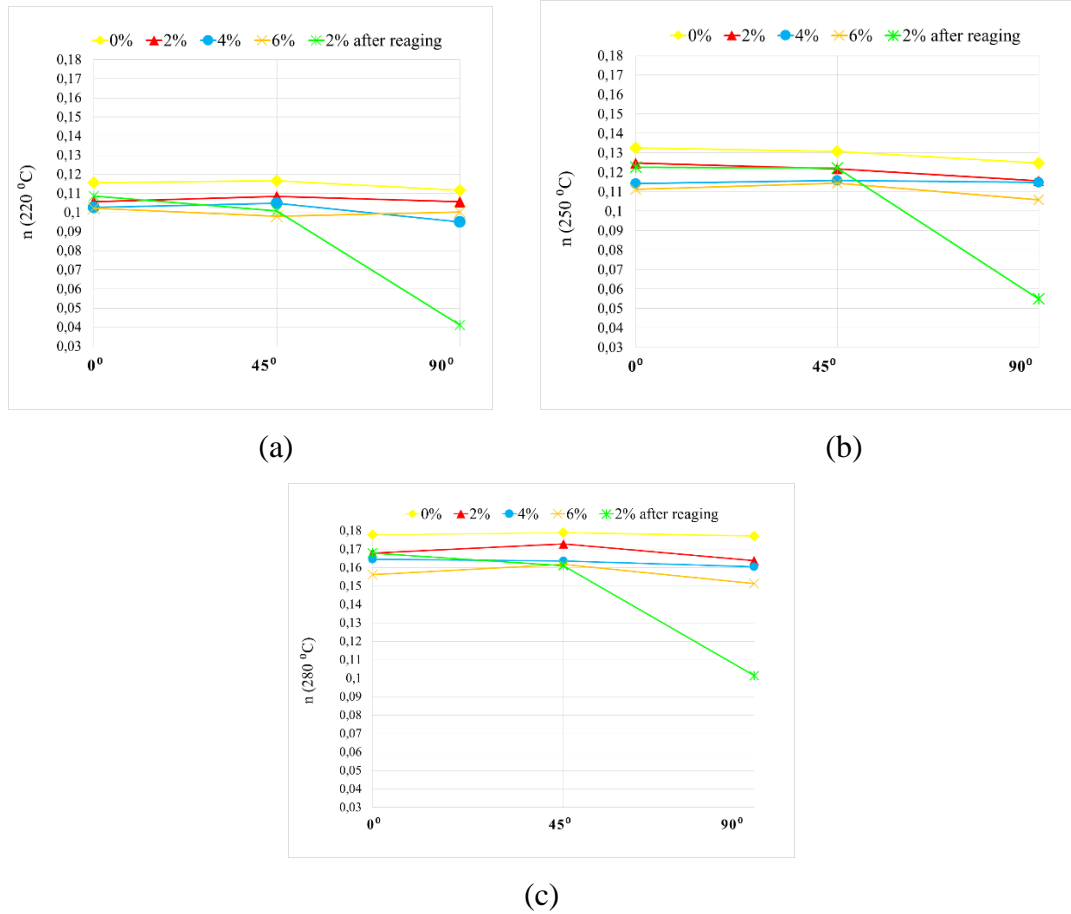
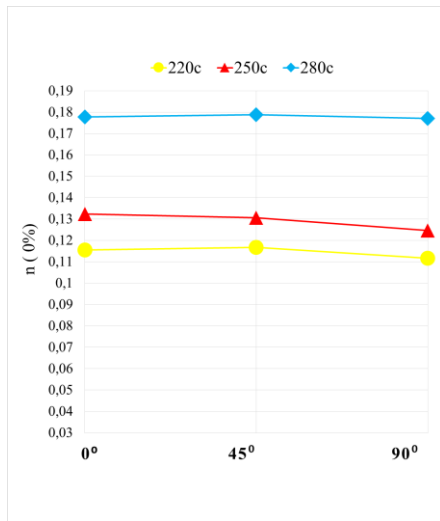
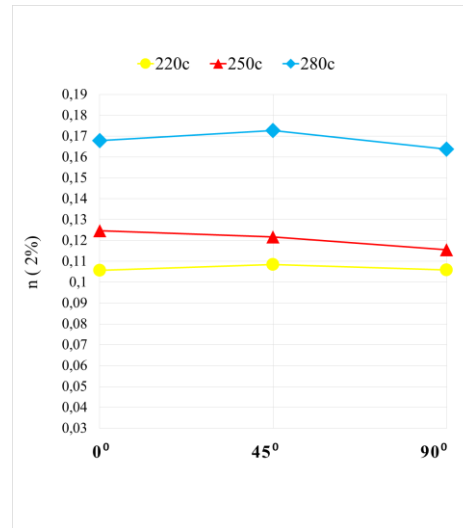


Figure 5.9 : Variation of strain hardening exponent with respect to sample orientation for different intermediate deformations for the samples retrogressed at (a) 220°C, (b) 250°C and (c) 280°C.

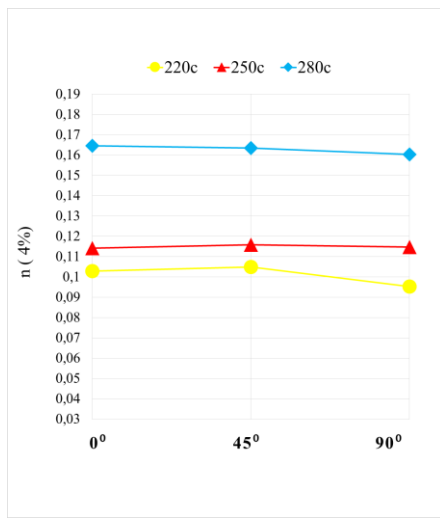
Figure 5.10a to e shows variation of strain hardening exponent with respect to sample orientation. It is clear that there is no clear difference between the strain hardening exponent values of the undeformed sample (Fig. 5.10a) and deformed samples (Fig. 5.10b to e). Also, strain hardening exponent values show almost no change with respect to sample orientation. It is only visible from Fig. 5.10 that strong effect of the highest retrogression temperature of 280°C in increasing strain hardening exponent values for all sample orientations.



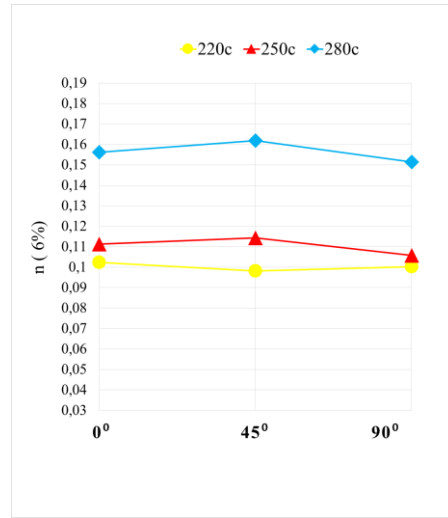
(a)



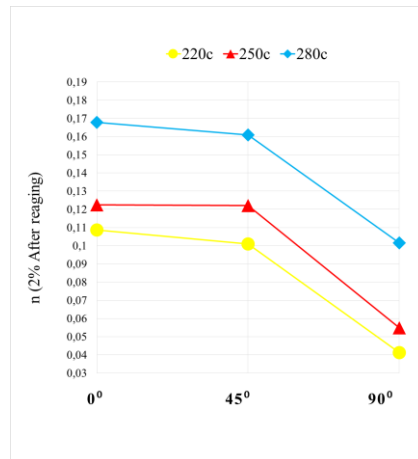
(b)



(c)



(d)



(e)

Figure 5.10 : Variation of strain hardening exponent with respect to sample orientation for different retrogression temperatures for the intermediate deformations of (a) 0% (undeformed), (b) 2%, (c) 4%, (d) 6% (e) RRA2%.

5.1.2.3 Effect of temperature

Figure 5.11 shows variation of strain hardening exponent with respect to retrogression temperature for different intermediate deformations. It is very apparent that retrogression temperature has a strong effect on strain hardening exponent. When the retrogression temperature increases, strain hardening exponent also increases accordingly. The highest strain hardening exponent values were obtained from the samples retrogressed at the highest retrogression temperature in this study (280°C). This may be related to the dislocation precipitate interaction during deformation. It suggests that precipitates in the microstructure which were slightly overaged when the retrogression temperature increases, are more effective to inhibit dislocation movement.

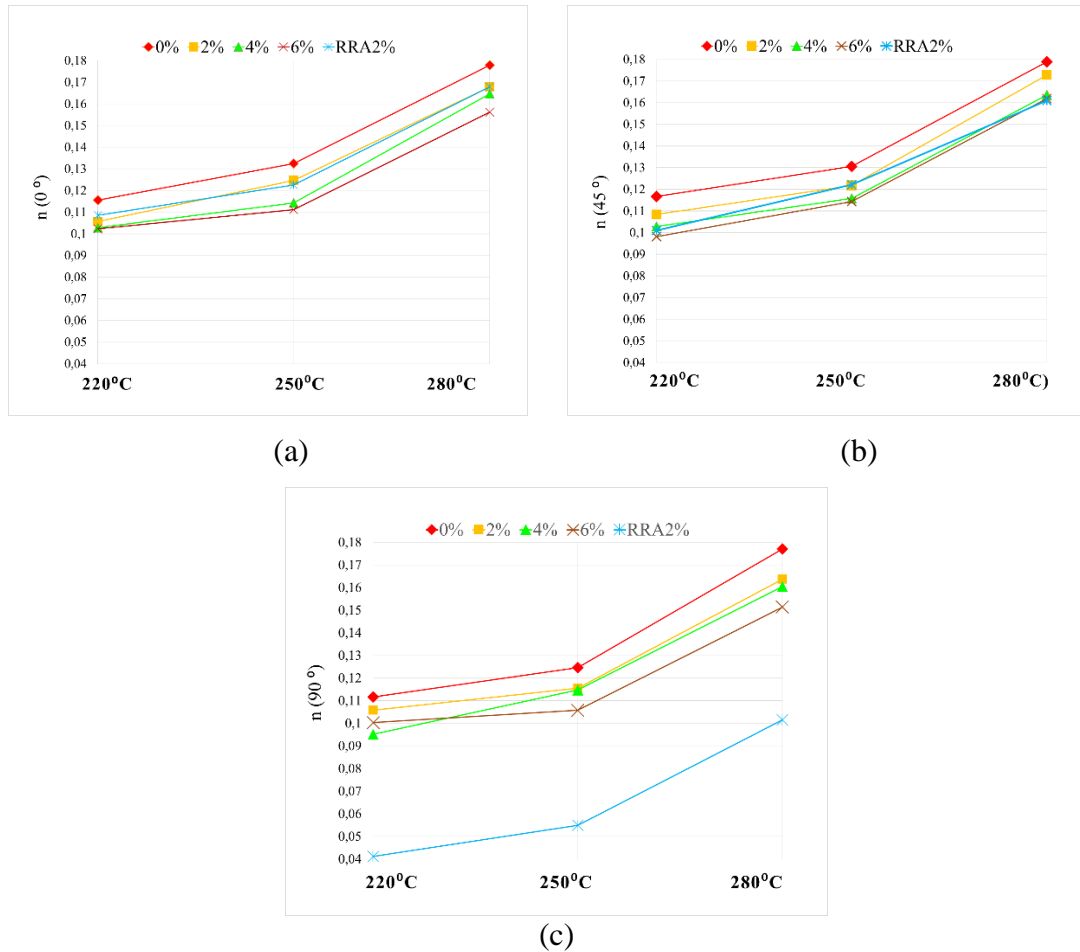


Figure 5.11 : Variation of strain hardening exponent with respect to retrogression temperature for different intermediate deformations for the sample orientations of (a) 0°, (b) 45° and (c) 90°.

Figure 5.12 shows variation of strain hardening exponent with respect to retrogression temperature for different sample orientations. Strain hardening exponent increases with increasing retrogression temperature in a similar manner regardless of the intermediate deformation and the sample orientation. On the other hand, increasing of strain hardening exponent with respect to retrogression temperature is getting slower (exhibit smaller slope) when the sample was deformed 2% after reaging (Fig. 5.12e).

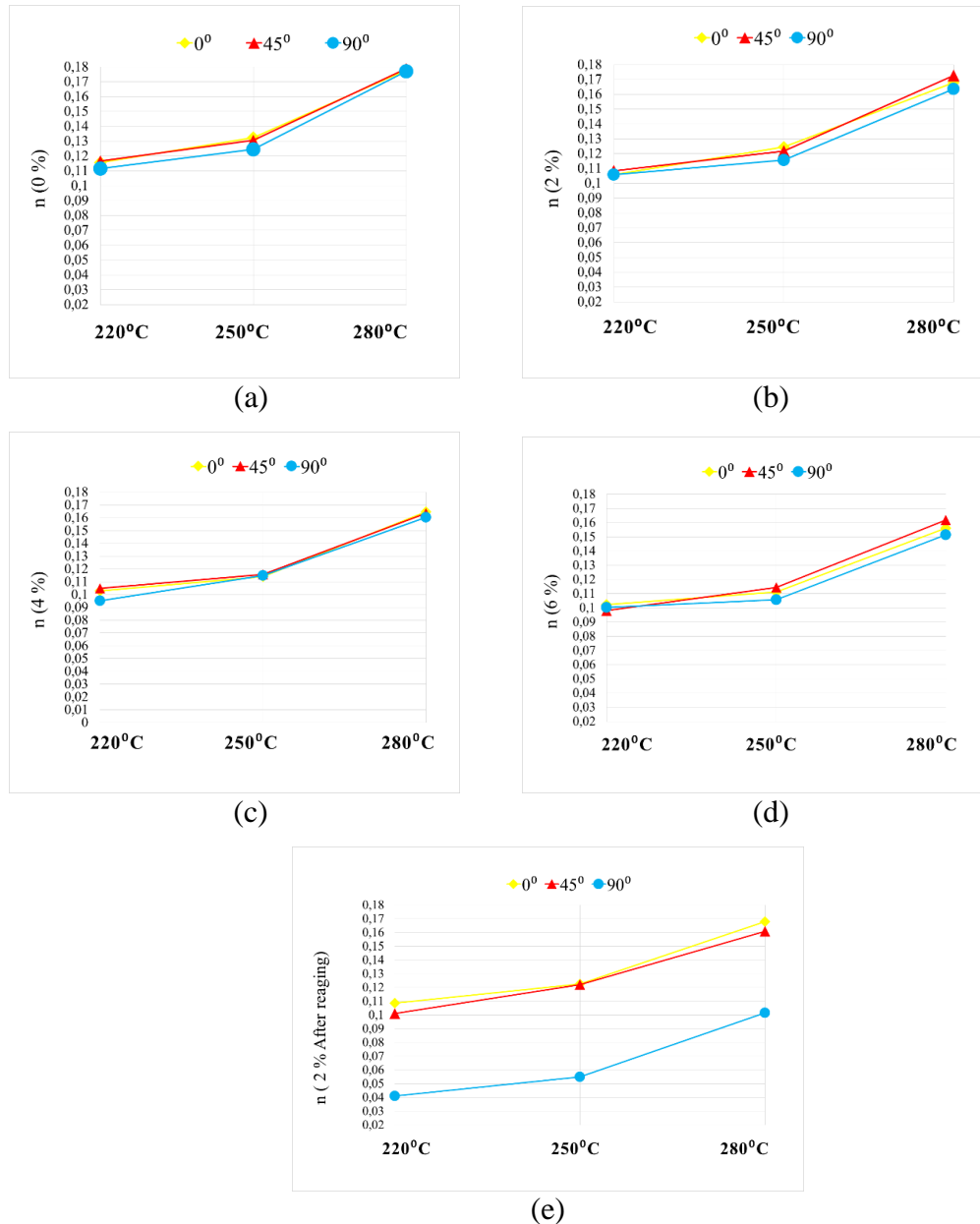


Figure 5.12 : Variation of strain hardening exponent with respect to retrogression temperature for different sample orientations for the intermediate deformations of (a) 0% (undeformed), (b) 2%, (c) 4%, (d) 6% (e) RRA2%.

5.1.3 Result of anisotropy coefficient (R)

Figure 5.13 and 5.14 shows variation of anisotropy coefficient with respect to sample orientation and intermediate deformation for different retrogression temperatures. It is clear from Fig. 5.13 that anisotropy coefficient is higher for the samples oriented 45° to the rolling direction than those oriented 0° and 90° . However, there is no simple relationship between the anisotropy coefficient and retrogression temperature. On the other hand, anisotropy coefficient exhibited a decreasing trend with respect to the increasing intermediate deformation. It is more apparent that for the retrogression temperatures of 220°C and 280°C .

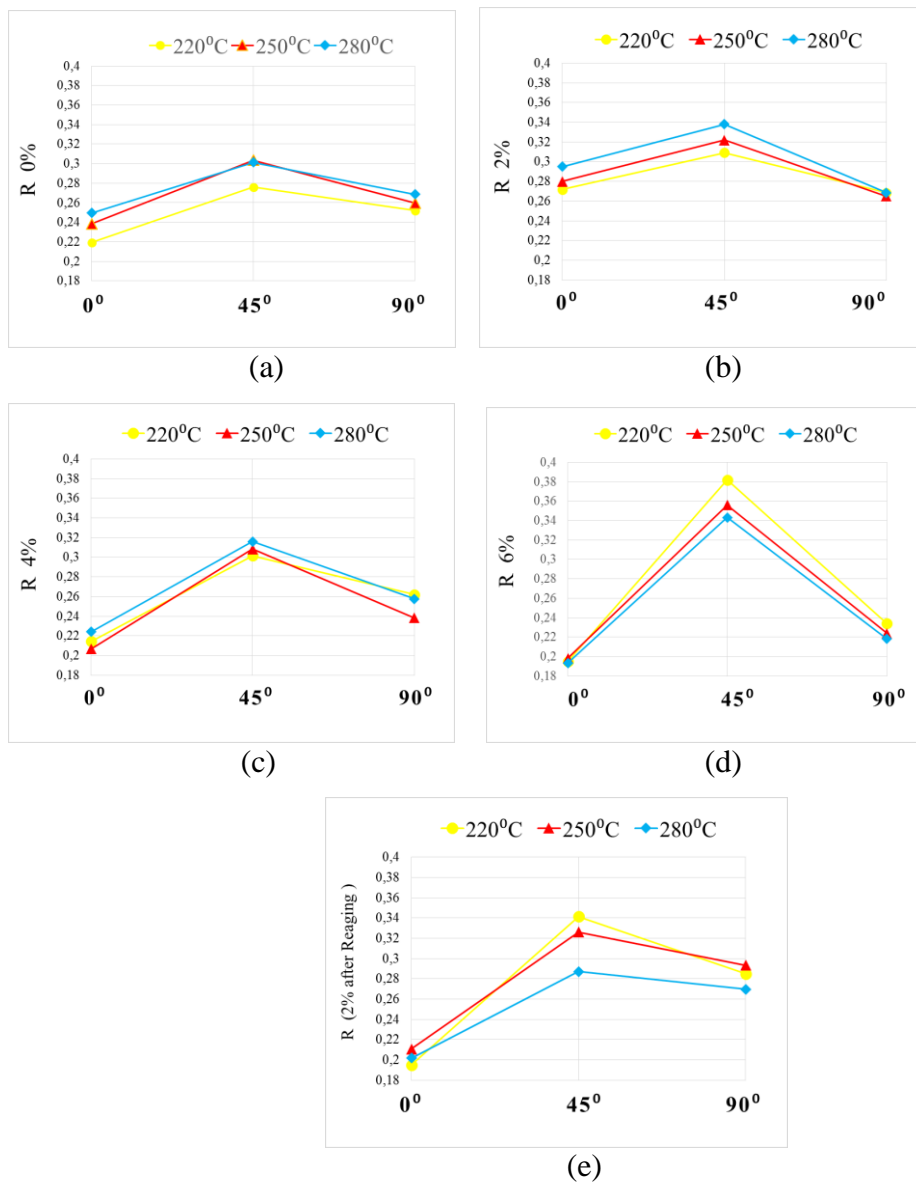


Figure 5.13 : Variation of anisotropy coefficient with respect to sample orientation for different retrogression temperatures for the intermediate deformations of (a) 0% (undeformed), (b) 2%, (c) 4%, (d) 6% (e) RRA2%.

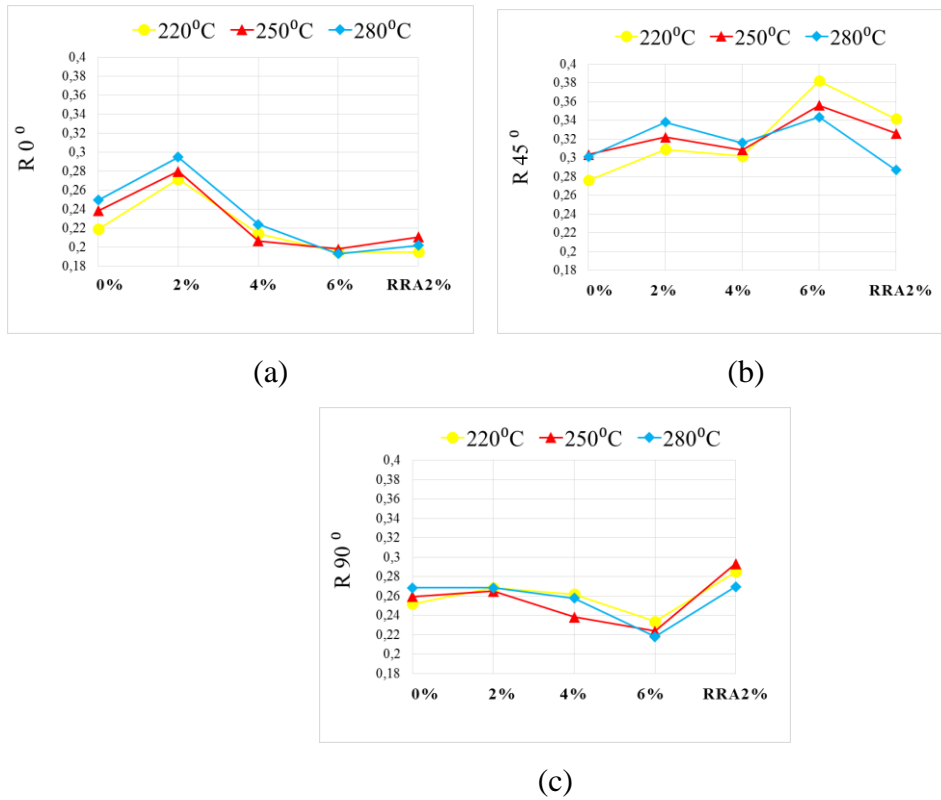


Figure 5.14 : Variation of anisotropy coefficient as a function of intermediate deformation for different retrogression temperatures for the sample orientations of (a) 0°, (b) 45° and (c) 90°.

5.2 Hardness Tests

Figure 5.15 shows hardness variation of the sample with respect to intermediate deformation for different retrogression temperatures. It should be first mentioned that there is no significant variation with respect to the intermediate deformation. However, hardness decreases with increasing retrogression temperature.

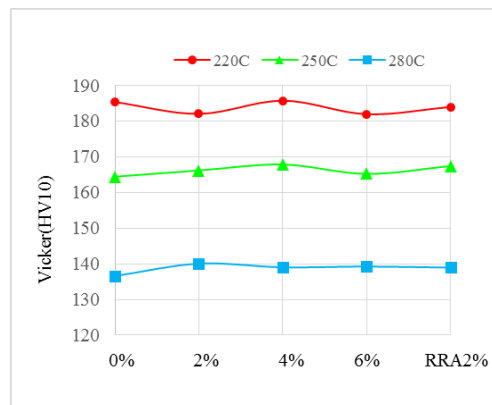


Figure 5.15 : Variation of hardness with respect to intermediate deformation for different retrogression temperatures.

5.3 Electrical Conductivity Measurements

Figure 5.16 shows variation of electrical conductivity with respect to intermediate deformation for different retrogression temperatures. As previously mentioned, electrical conductivity is a good indicator of corrosion resistance of the samples. As electrical conductivity increases, corrosion resistance increases accordingly. It is apparent from Fig. 5.16 that there is no significant variation in electrical conductivity of the samples with intermediate deformation. However, electrical conductivity increases with increasing retrogression temperature. This indicates that corrosion resistance also increases with increasing retrogression temperature, as expected.

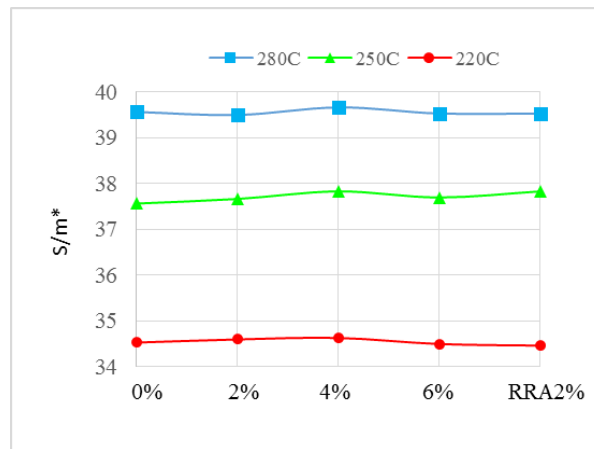


Figure 5.16 : Variation of electrical conductivity with respect to intermediate deformation for different retrogression temperatures.

5.4 Comparison of experimental results of 7075-T6 and 7075-RRA alloys

Table 5.1 summarizes all mechanical test results obtained from the undeformed samples. As can be seen from Table 5.1, tensile test results such as yield strength, ultimate tensile strength, elongation at fracture and hardness all decrease upon application of retrogression and reaging heat treatment. Similarly, anisotropy coefficient values also decreased. On the other hand, strain hardening exponent and electrical conductivity values continuously increase with increasing retrogression temperature. When the strength and formability values are considered together, retrogression temperature of 250°C gives optimum retrogression temperature. At this temperature hardness and strength values decreased 17% and about 10%, respectively, while strain hardening exponent increased about 65%.

Table 5.1.Comparison of mechanical test results

			e%		σ _y		σ _{max}		R		n		HV(10)		R _{average}		ΔR		Electrical Conductivity
Original	0°		11,3		510		573		0,57		0,079								
Original	45°		11,9		482		561		0,54		0,077		198		0,526		-0,121		31,5
Original	90°		11,5		506		570		0,55		0,078								
220° C	0°	0%	10,9	-3,5%	321	-37%	424	-26%	0,24	-57%	0,115	45%							
220° C	45°	0%	12,2	2,5%	320	-33%	433	-22%	0,33	-38%	0,116	50%	185	-6%	0,277	-47%	-0,08	34,53	9%
220° C	90°	0%	10,9	-5,2%	324	-35%	435	-23%	0,27	-50%	0,111	42%					54%		
250° C	0°	0%	11,5	1,7%	419	-17%	506	-11%	0,24	-57%	0,132	68%							
250° C	45°	0%	12,5	5%	417	-13%	504	-10%	0,35	-35%	0,13	68%	164	-17%	0,286	-45%	-0,033	37,56	19%
250° C	90°	0%	9,7	-15%	429	-15%	509	-10%	0,26	-52%	0,124	58%					72%		
280° C	0°	0%	10,9	-3,5%	324	-36%	437	-23%	0,23	-57%	0,177	124%							
280° C	45°	0%	12,2	2,5%	317	-34%	429	-23%	0,24	-55%	0,178	131%	136	-31%	0,263	-50%	-0,009	39,5	25%
280° C	90°	0%	10,9	-5,2%	322	-36%	438	-23%	0,25	-54%	0,177	126%					92%		

6. CONCLUSION

In this study, effect of intermediate deformation on hardness, strength and formability parameters of retrogressed and reaged 7075 aluminum alloy was investigated and the following conclusions were obtained:

1. Hardness of samples decreases with increasing retrogression temperature. Highest hardness was obtained from the retrogression temperature of 220°C as 185 HV10 for undeformed sample. for the sample temperature and 220°C has the highest hardness.
2. Yield strength and ultimate tensile strength both decreases with increasing retrogression temperature. Highest values of yield and tensile strength were obtained from the retrogression temperature of 250°C as 429 MPa and 509 MPa, respectively.
3. With increasing retrogression temperature, strain hardening exponent (n) increases with increasing retrogression temperature. The highest value of n is obtained from the retrogression temperature of 280°C as 0.179 for undeformed sample.
4. Anisotropy coefficient increases with increasing retrogression temperature. Highest average (normal) anisotropy coefficient was obtained from the retrogression temperature of 280°C as 0.286 for undeformed sample.
5. Electrical conductivity increases with increasing retrogression temperature.
6. Intermediate deformation has not any significant effect on hardness, strain hardening exponent, anisotropy coefficient and electrical conductivity.
7. Orientation of the samples to the rolling direction has not a significant effect of strain hardening exponent.
8. When strength values and strain hardening exponent are considered together, retrogression temperature of 250°C is the optimum retrogression temperature.

REFERENCES

- [1] **Chen, L.G., Lin, S.J., Chang, S.Y.,** (2005). Analysis of interfacial shear strength of SiC fiber reinforced 7075 aluminum composite by pushout microindentation, *Metallurgical and Materials Transactions A: Physical Metallurgy and Materials Science*, 36, 7, 1937–45.
- [2] **Choudhry, M.A., Ashraf, M.,** (2006). Effect of heat treatment and stress relaxation in 7075 aluminum alloy, *Journal of Alloys and Compounds*, 437, 1–2, 113–116.
- [3] **Rometsch, P.A., Zhang, Y., Knight, S.,** (2013). Heat treatment of 7xxx series aluminum alloys—Some recent developments, *Transactions of Nonferrous Metals Society of China*, 24, 7, 2003–2017.
- [4] **Spigarelli, S., Evangelista, E., Cerri, E.,** (2001). Constitutive equations for hot deformation of an Al-6061/20%Al₂O₃ composite, *Material Science Engineering A*, 319–321, 721–726.
- [5] **Wannasin, J., Janudom, S., Rattanochaikul, T., Canyook, R., Burapa, R., Chuchee, T., Thanabumrungkul, S.,** (2010). Research and development of gas induced semi-solid process for industrial applications, *Transactions of Nonferrous Metals Society of China*, 20, 1010-1015.
- [6] **Thanabumrungkul, S., Janudom, S., Burapa, R., Dulyapraphant, P., Wannasin, J.,** (2010). Industrial development of gas induced semi-solid process, *Transactions of Nonferrous Metals Society of China*, 20, 1016-1021.
- [7] **Clark, R.Jr., Coughran, B., Traina, I., Hernandez, A., Scheck, T., Etuk, C., Peters, J., Lee, E.W., Ogren, J., Es-Said, O.S.,** (2005). On the correlation of mechanical and physical properties of 7075-T6 Al alloy, *Engineering Failure Analysis*, 12, 4, 497-652.
- [8] **Song, M., Chen, K.,** (2008). Effects of the enhanced heat treatment on the mechanical properties and stress corrosion behavior of an Al–Zn–Mg alloy, *Journal of Materials Science*, 43, 15, 5265-5273.
- [9] **ASM Metals Handbook.** (1991). *Heat Treating*, Vol. 4, ASM International, Materials park, Ohio, USA.
- [10] **Mukhopadhyay, P., Samajdar, I.,** (2008). Sources of recrystallized grains and their contributions in recrystallization of an AA3104 aluminum alloy, *Transactions of the Indian Institute of Metals*, 61, 4, 329-339.
- [11] **Mahathaninwong, N., Plookphol, T., Wannasin, J., Wisutmethangoon, S.,** (2012). T6 heat treatment of rheocasting 7075 Al alloy, *Materials Science and Engineering A*, 532, 91–99.

- [12] **Williams, J.C., Starke, E.A.,** (2003). Progress in structural materials for aerospace systems, *Acta Materiala*, 51, 19, 5775–5799.
- [13] **Cina, B.,** (1974). Reducing the Susceptibility of Alloys, Particularly Aluminum, to Stress Corrosion Cracking: US Patent, 3856584.
- [14] **Oliveira, A.F.Jr., de Barros, M.C., Cardoso, K.R., Travessa, D.N.,** (2004). The effect of RRA on the strength and SCC resistance on AA7050 and AA7150 aluminum alloys, *Materials Science and Engineering A*, 379, 1-2, 321-326.
- [15] **Li, G-f., Zhang, X-m., Li, P-h., You, J-h.,** (2010). Effects of retrogression heating rate on microstructures and mechanical properties of aluminum alloy 7050. *Transactions of Nonferrous Metals Society of China*, 20, 6, 935-941.
- [16] **Cobden, R.,** (1994). Physical Properties, Characteristics and Alloys, *European Aluminum Association*, Brussels.
- [17] **Url-1** <http://en.wikipedia.org/wiki/Aluminum_alloy>.
- [18] **Kaufman, J.G.,** (2000). Introduction to Aluminum Alloys and Tempers. *A S M International*, 2000. Materials Park, OH, USA
- [19] **Url-2** <<http://www.esab.ca/ca/en/education>>, date retrieved 12.10.2014.
- [20] **Gitter, R.,** (2008). Design of aluminum structure: selection of structure alloys, *EUROCODES-Background and application*, Brussels.
- [21] **Url-3** <<http://www.esab.ca/ca/en/education>>, date retrieved 05.08.2014.
- [22] **Url-4** <<http://www.chemistryexplained.com>>, date retrieved 08.11.2014.
- [23] **Tajally, M., Huda, Z., Masjuki, H.H.,** (2010). A comparative analysis of tensile and impact-toughness behavior of cold-worked and annealed 7075 aluminum alloy, *International Journal of Impact Engineering*, 37, 4, 425–432.
- [24] **Yang, Y., Xie, Z.P., Zhang, Z., Li, X., Wang, Q., Zhang, Y.,** (2014). Processing maps for hot deformation of the extruded 7075 aluminum alloy bar: Anisotropy of hot workability. *Materials Science and Engineering A*, 615, 183-190.
- [25] **Mahathaninwong, N., Zhou, Y., Babcock, S.E., Plookphol, T., Wannasin, J., Wisutmethangoon, S.,** (2012). Creep rupture behavior of semi-solid cast 7075-T6 Al alloy, *Materials Science and Engineering A*, 566, 107-113.
- [26] **Feng, C., Liu, Z., Ning, A-l., Liu, Y-b,** (2006). Retrogression and re-aging treatment of Al-9.99%Zn- 1.72%Cu-2.5%Mg-0.13%Zr aluminum alloy, *Transactions of Nonferrous Metals Society of China*, 16, 1163-1170.
- [27] **El-Amoush, A.S.,** (2008). An investigation of hydrogen-induced hardening in 7075-T6 aluminum alloy, *Journal of Alloys and Compounds*, 465, 1–2, 497–501.
- [28] **Ortiz, D., Abdelshehid, M., Dalton, R., Soltero, J., Clark, R., Hahn, M., Lee, E., Lightell, W., Pregger, B., Ogren, J., Stoyanov, P. Es-Said, O.S.,** (2007). Effect of cold work on the tensile properties of

- 6061, 2024, and 7075 Al alloys, *Journal of Materials Engineering and Performance*, 16, 5, 515-520.
- [29] **Reda, Y., Abdel-Karim, R., Elmahallawi, I.**, (2008). Improvements in mechanical and stress corrosion cracking properties in Al-alloy 7075 via retrogression and reaging, *Materials Science and Engineering: A*, 485, 1–2, 468–475.
 - [30] **Papazian, J.M.**, (1986). Differential scanning calorimetry evaluation of retrogressed and re-aged microstructures in aluminum alloy, *Material Science Engineering*, 97, 1, 97-104.
 - [31] **Ward, N., Tran, A., Abad, A., Lee, E.W., Hahn, M., Fordan, E., Es-Said O.S.**, (2011). The Effects of Retrogression and Reaging on Aluminum Alloy 2099 (C458), *Journal of Materials Engineering and Performance*, 20, 6, 989-996.
 - [32] **Viana, F., Pinto, A.M.P., Santosa H.M.C., Lopes, A.B.**, (1999). Retrogression and re-ageing of 7075 aluminum alloy: microstructural characterization, *Journal of Materials Processing Technology*, 92-93, 54-59.
 - [33] **Umamaheshwer Rao, Vasu, V., Govindaraju, M., Sai Srinadh, K.V.**, (2014). Influence of Cold Rolling and Annealing on the Tensile Properties of Aluminum 7075 Alloy, *Procedia Materials Science*, 5, 86–95.
 - [34] **Ohnishi, T., Shiota, H.**, (1986). Heat treatment to reduce the susceptibility of Al-Zn-Mg-Cu alloy to stress corrosion cracking, *Journal of Japan Institute of Light Metals*, 36, 10, 647-656.
 - [35] **Hwang, R.Y., Chou, C.P.**, (1997). The study on microstructural and mechanical properties of weld heat affected zone of 7075-T651 aluminum alloy, *Scripta Materialia*, 38, 2, 215–221.
 - [36] **Islam, M.U., Wallace, W.**, (1983). Retrogression and Reaging Response of 7475 Aluminum Alloy, *Metals Technology*, 10, 1, 386-392.
 - [37] **Jaburek, N., Merklein, M.**, (2013). Study of a formability process chain for a copper-free Al-Zn-Mg-alloy by a retrogression and re-aging treatment (RRA), *Key Engineering Materials*, 549, 295-301.
 - [38] **Peng, G-S., Chen, K-h., Chen, S-y., Fang, H-c.**, (2012). Influence of dual retrogression and re-aging temper on microstructure, strength and exfoliation corrosion behavior of Al-Zn-Mg-Cu alloy, *Transactions of Nonferrous Metals Society of China*, 22, 4, 803-809.
 - [39] **Hepples, W., Jarrett, M.R., Crompton, J.S., Holroyd, N.J.H.**, (1988). Influence of microstructure on the stress corrosion cracking and exfoliation of commercial Al-Zn-Mg-Cu alloys, *International Corrosion Conference Series NACE*, 10, 383-388.
 - [40] **Feng, D., Zhang, X.M., Liu, S.D., Deng, Y.L.**, (2014) Non-isothermal retrogression and re-ageing treatment schedule for AA7055 thick plate, *Materials and Design*, 60, 208–217
 - [41] **Angappan, M., Sampath, V., Ashok, B., Deepkumar, V.P.**, (2011). Retrogression and re-aging treatment on short transverse tensile

properties of 7010 aluminum alloy extrusions, *Materials and Design*, 32, 7, 4050–4053.

- [42] **Gao, M., Feng, C.R., Wei, R.P.**, (1998). An analytical electron microscopy study of constituent particles in commercial 7075-T6 and 2024-T3 alloys, *Metallurgical and Materials Transactions A*, 29, 4, 1145-1151.
- [43] **Oskoue, R.H., Ibrahim, R.N.**, (2011). The effect of a heat treatment on improving the fatigue properties of aluminum alloy 7075-T6 coated with TiN by PVD, *Procedia Engineering*, 10, 1936–1942.
- [44] **Wang, Y.L., Pan, Q.L., Wei, L.L., Li, B., Wang, Y.**, (2014). Effect of retrogression and reaging treatment on the microstructure and fatigue crack growth behavior of 7050 aluminum alloy thick plate, *Materials and Design*, 55, 857–863.
- [45] **Lechner, M., Johannes, M., Kuppert, Merklein, M.**, (2014). Influence of pre-straining and heat treatment on the yield surface of precipitation hardenable aluminum alloys, *Physics Procedia*, 56, 1400 – 1409.
- [46] Sha, G. **Cerezo, A.**, (2004). Characterization of precipitates in an aged 7xxx series Al alloy, *Surface and Interface Analysis*, 36, 5-6, 564-568.
- [47] **Xiao, Y-P., Pan, Q-L., Li, W-B., Liu, X-Y., He, Y-B.**, (2011). Influence of retrogression and re-aging treatment on corrosion behavior of an Al–Zn–Mg–Cu alloy, *Materials and Design*, 32, 4, 2149–2156.
- [48] **Buha, J., Lumley, R.N., Crosky, A.G.**, (2008). Secondary ageing in an aluminum alloy 7050, *Materials Science and Engineering A*, 492, 1-2, 1-10.
- [49] **Marlaud, T., Deschamps, A., Bley, F., Lefebvre, W., Baroux, B.**, (2010). Evolution of precipitate microstructures during the retrogression, re-aging heat treatment of an Al–Zn–Mg–Cu. Alloy, *Acta Materialia*, 58, 4814–4826.
- [50] **Arabi Jeshvaghani, R., Zohdi, H., Shahverdi, H.R., Bozorg, M., Hadavi, S.M.M.**, (2012). Influence of multi-step heat treatments in creep age forming of 7075 aluminum alloy: Optimization for springback, strength and exfoliation corrosion, *Materials Characterization*, 73, 8-15.
- [51] **Peng, G., Chen, K., Chen, S., Fang, H.**, (2011). Influence of repetitious-RRA treatment on the strength and SCC resistance of Al–Zn–Mg–Cu alloy. *Materials Science and Engineering: A*, 528, 12, 4014–4018.
- [52] **Cavanaugh, M.K., Birbilis, N., Buchheit, R.G., Bovard, F.**, (2007). Investigation localized corrosion susceptibility arising from Sc containing intermetallic Al₃Sc in high strength Al-alloys, *Scripta Materialia*, 56, 11, 995-998.
- [53] **Ranganatha, R., Anil Kumar, V., Nandi, V.S., Bhat, R.R., Muralidhara, B.K.**, (2013) Multi-stage heat treatment of aluminum alloy AA7049, *Transaction of Nonferrous Metals Society of China*, 23, 6, 1570-1575.
- [54] **Tobolski, E.L., Fee, A.**, (2000), Macroindentation Hardness Testing," *ASM Handbook*, Volume 8: Mechanical Testing and Evaluation, ASM International, pp. 203-211.

CURRICULUM VITAE



Name Surname:Armin RASHIDI

Place and Date of Birth: IRAN 29.01.1984

E-Mail: armin.rashidi31@gmail.com

B.Sc.: Civil Engineering

M.Sc.: Metallurgy and Materials Engineering